Title

Dissecting immune regulation and dysregulation in autoimmune diabetes from the vantage point of the target tissue

Permalink

https://escholarship.org/uc/item/48n2c0n8

Author

Mahne, Ashley

Publication Date

2013

Peer reviewed|Thesis/dissertation

DISSECTING IMMUNE REGULATION AND DYSREGULATION
IN AUTOIMMUNE DIABETES FROM THE VANTAGE POINT
OF THE TARGET TISSUE

by

Ashley Mahne

DISSERTATION

Submitted in partial satisfaction of the requirements for the degree of

DOCTOR OF PHILOSOPHY

in

Biomedical Sciences

in the

GRADUATE DIVISION

of the

UNIVERSITY OF CALIFORNIA, SAN FRANCISCO

ACKNOWLEDGEMENTS

more intellectually stimulating environment, while also being great people to work with. Deskmates Greg and Lindsay have been both helpful and a pleasure to be around on a daily basis. During my time in the lab, many people have come and gone. Some past members of the Transplant lab I would also like to acknowledge for their support are Ninnia, Clara, Harras, Susannah, and Anne.

I'd like to thank the members of my thesis committee, Jason and Jeff, for making committee meetings something to look forward to. Their much-appreciated input and advice along the way were essential in shaping this work.

Members of other labs at UCSF have also provided help and inspiration along the way. Members of the Bluestone, Anderson, Abbas, Rosenblum and Mackenzie labs have been wonderful to interact with at weekly lab meetings and beyond. I'd also like to thank the Krummel lab for giving me a great first introduction to UCSF, especially Julia, Emily and Rachel.

Thank you to members of the BMS office, especially Lisa and Monique, for taking care of so many things for me that I didn't even know about.

I feel very blessed to have made such good friends in San Francisco that have brought immeasurable joy to these past years. Thank you to friends in the BMS program, especially Robyn, Yelena, Julie, and Mike. Being able to share successes and good times and to sometimes commiserate with you has been essential to getting through this process. Thank you to Nicole, Aaron, Erin, Emily, Greg, Emily, Edith, and Brendan for countless fun days and nights and for being great friends.

I have been blessed with exceptional in-laws. Thank you to the Mahne family for welcoming me as one of your own and being so supportive of everything I do.

My mom and dad are the reason I am who I am today, and I am forever grateful. They have always believed in me and supported me, even when it meant watching me go to faraway places. My sisters, Taylor and Hillary, have also shaped me in countless ways. I love you all.

Forever thank yous to my husband and best friend, Brandon. Coming home to you, Obi, and Marcel every night is what makes everything worthwhile. Thank you for loving me unconditionally, for making each day better than the last, for being my steadfast partner in all of life's adventures. I love you.

CONTRIBUTIONS OF CO-AUTHORS TO THE PRESENTED WORK

Chapter II of this dissertation is based on a manuscript in submission as "Regulatory T cells exert multi-level suppression of $CD8^+$ T cells in the target tissue in autoimmune diabetes." The co-authors on this publication will be Annie Chou[1], Vinh Nguyen[1] and Qizhi Tang[1]. Annie Chou provided technical assistance. Vinh Nguyen performed mouse islet isolations and provided technical assistance. Qizhi Tang supervised the work.

Chapter III of this dissertation is based on a manuscript in preparation. The co-authors on the resulting publication will be Joanna Klementowicz[1], Annie Chou[1], Vinh Nguyen[1], Mariela Pauli[2] and Qizhi Tang[1]. Joanna Klementowicz, Annie Chou, and Mariela Pauli provided assistance with experiments. Vinh Nguyen performed mouse islet isolations and provided technical assistance. Qizhi Tang supervised the work.

[1]Department of Surgery, University of California, San Francisco, San Francisco, CA

[2]Department of Dermatology, University of California, San Francisco, San Francisco, CA

DISSECTING IMMUNE REGULATION AND DYSREGULATION IN AUTOIMMUNE DIABETES FROM THE VANTAGE POINT OF THE TARGET TISSUE

Ashley Mahne

ABSTRACT

Regulatory T cells (Tregs) are critical to the maintenance of immune homeostasis and the prevention of autoimmunity. In the NOD mouse model of autoimmune diabetes, treatment with therapeutic Tregs can prevent and even reverse disease onset. The means by which Tregs are able to exert their protective effects *in vivo* have remained incompletely understood. This work focused on elucidating the critical cellular targets of Tregs at the site of inflammation and the effects of Tregs on these target cells. This was accomplished by examining the target tissue, the pancreatic islets of Langerhans, before and after Treg treatment with a variety of approaches. Islets and their immune infiltrates were analyzed at the transcriptional and post-transcriptional levels. Islet immune infiltrates were characterized at the phenotypic and functional levels by flow cytometry and by multiple modes of microscopic imaging. Therapeutic Tregs were found to quickly home to inflamed islets, where they engaged in dynamic interactions with resident dendritic cells (DCs). Treg arrival was followed by a rapid decrease in islet $CD8^+$ T cells that corresponded with a reduction in the expression of cytotoxic effectors and cytokines. T cells that persisted in the islets following Treg treatment showed no decrease in

proliferative capacity but were suppressed at the level of effector function, where they lacked production of IFNγ protein despite continued expression of IFNγ mRNA. In CD8$^+$ T cells, this inhibition of effector function was related to a decrease in mTOR signaling that was required for sustained IFNγ production. In addition to these acute effects on CD8$^+$ T cells following Treg treatment, we also observed a more gradual impact on islet DCs. The recruitment of DCs was reduced in the weeks following Treg treatment. Islet DCs were found to arise from a blood monocyte precursor. Overall, our findings that therapeutic Tregs target CD8$^+$ T cells during acute disease control and DCs during later stages implicate the importance of these targets in disease pathogenesis and elucidates the mechanisms by which therapeutic Tregs exert their protective effects.

TABLE OF CONTENTS

Chapter I:

Introduction

Chapter II:

Regulatory T cells exert multi-level suppression of CD8$^+$ T cells in the target tissue in autoimmune diabetes

Chapter III:

Recruitment of dendritic cells to inflamed islets and the effects of therapeutic Tregs

Chapter IV:

Conclusions and future directions

LIST OF TABLES

CHAPTER II

LIST OF FIGURES

CHAPTER II

CHAPTER III

CHAPTER I: INTRODUCTION

Autoimmunity: The cost of an adaptive immune system

In higher vertebrates, adaptive immunity has arisen to provide highly specialized protection against pathogens. The adaptive arm of the immune system is comprised of T and B lymphocytes that undergo selection for their expression of receptors that recognize specific antigens. In the context of a pathogenic infection, a lymphocyte that recognizes pathogen-derived antigen will undergo clonal expansion, producing large numbers of daughter cells to eliminate the pathogen. Following resolution of an infection, the majority of these lymphocytes will die, but a small subset will become memory cells that persist long term, providing rapid protection if the same pathogen is encountered again.

Key to the proper function of adaptive immunity is the maintenance of immune tolerance, or the prevention of reactivity to self-antigens. Immune tolerance can be divided into two categories: central and peripheral tolerance. Central tolerance acts during the development of T and B cells. Cells that react too strongly against self-antigens are deleted by negative selection. As not all self-antigens are presented during lymphocyte development and negative selection can at times be incomplete, peripheral tolerance acts as a backup to central tolerance, suppressing activation in the periphery of self-reactive cells.

The concept of autoimmunity, or an immune response directed against self, was first proposed at the turn of the 20th century by the German physician-scientist Paul Ehrlich. Ehrlich referred to the idea of self-reactivity as "horror autotoxicus," which he

believed to be incompatible with life because of its potentially devastating consequences to the organism. Advances in our understanding of the immune system have shown however that a number of autoimmune diseases do in fact exist, which result in organ-specific or systemic immune-mediated damage in the host. Some of the most common autoimmune diseases include type 1 diabetes (T1D), rheumatoid arthritis (RA), systemic lupus erythromytosis (SLE), Sjogren's syndrome, celiac disease and multiple sclerosis (MS) (McGonagle and McDermott, 2006). These disorders differ in the tissues they affect and their modes of pathogenesis, but share the common feature of being driven by a breakdown in immune tolerance that leads to activation of self-reactive adaptive immune cells.

Regulatory T cells: Enforcers of peripheral tolerance

Paramount in the maintenance of peripheral tolerance are regulatory T cells (Tregs). Tregs are specialized T cells that function to suppress immunity. The study of Tregs exploded in 2003 with the discovery of Foxp3 as the master transcription factor for these cells (Fontenot et al., 2003; Hori et al., 2003; Khattri et al., 2003). Immunologists had long suspected that such suppressive T cells existed. The study of suppressor T cells began in the 1970s, but the lack of specific markers to identify these cells and problems with reproducing results obtained from complex experimental systems led to the demise of the field. Resurrection came in the 1990s, when Sakaguchi and colleagues described a subpopulation of CD4$^+$ T cells that expressed high levels of CD25 and had suppressive capabilities (Sakaguchi et al., 1995). As CD25 is also expressed on activated effector T

cells, it was an imperfect marker, but interest in the field was renewed. The search for a more definitive marker of this suppressive cell population was launched, and in 2003, 3 groups published the discovery of Foxp3 as the master Treg transcription factor nearly simultaneously (Fontenot et al., 2003; Hori et al., 2003; Khattri et al., 2003).

Foxp3 is essential to the stability and suppressive functions of Tregs. Genetic deletions or mutations of the Foxp3 gene in mice and humans neutralize these cells and illustrate the critical role of Tregs in the maintenance of immune homeostasis. In humans, mutations in the Foxp3 gene result in a syndrome referred to as immunodysregulation polyendocrinopathy enteropathy X-linked syndrome, or IPEX syndrome. This often-fatal disease is characterized by systemic autoimmunity targeting a number of tissues, including organs of the endocrine system and skin (van der Vliet and Nieuwenhuis, 2007). Similarly in mice, the scurfy mutation leads to a loss of Foxp3 and results in early-onset, fatal, multi-organ autoimmunity (Brunkow et al., 2001). Tregs can be broadly divided into two main categories: natural and adaptive. Natural Tregs are generated in the thymus and express Foxp3 from the time of their selection. In contrast, adaptive Tregs arise in the periphery from naïve CD4$^+$ T cells that are activated in the context of tolerogenic signals that trigger *de novo* expression of Foxp3 and adoption of a suppressive phenotype.

In addition to their essential role in maintaining immune homeostasis, proper Treg function is also key to a balanced immune response (Sakaguchi, 2004). In the setting of cancer for example, overly active Tregs can inhibit desired effector T cell clearance of tumor cells and promote disease progression. In infections, Tregs can prevent immune responses from becoming damaging to the host. In some cases, this comes with the

trade-off of incomplete pathogen clearance leading to chronic infection. In contrast, deficits in Treg responses can lead to settings of chronic inflammation and have been linked to autoimmunity.

Initially, Tregs were believed to be anergic and refractory to proliferation *in vitro* (Sakaguchi, 2004). However, Tregs sorted from the secondary lymphoid organs of mice or the peripheral blood of humans, primarily on the basis of CD4 and CD25 expression, can be expanded to large numbers and maintain suppressive function when cultured with anti-CD3 and anti-CD28 stimulation in the presence of high levels of IL-2 (Putnam et al., 2009; Tang et al., 2004). These discoveries allowed researchers to obtain large numbers of these cells to study, despite their normally low frequency (less than 2% of peripheral blood T cells). Adoptive transfer experiments using *in vitro* expanded Tregs have shown the suppressive capabilities of these cells *in vivo*. In mouse models, Treg treatment suppresses GVHD, transplant rejection, and a number of autoimmune conditions, including inflammatory bowel disease, arthritis, SLE, EAE, and T1D (discussed in more detail below) (Tang and Bluestone, 2006).

A number of mechanisms have been described for how Tregs exert their suppressive effects (Vignali et al., 2008). CTLA-4 is highly expressed on the surface of Tregs, and this expression is essential for the maintenance of immune homeostasis (Wing et al., 2008). In many settings of immune activation however, CTLA-4 expression does not always appear to be required for suppressive Treg function. Other mechanisms demonstrated *in vivo* to play a role in the suppressive function of Tregs includes the secretion of suppressive cytokines such as IL-10, TGFβ and IL-35, the killing of target cells by granzyme and perforin, and the deprivation of IL-2 from IL-2-dependent effector

T cells (Yamaguchi et al., 2011).   The specific requirements for each of these mechanisms in different settings remains incompletely understood and are likely context dependent.

T1D and the NOD mouse model of autoimmune diabetes

T1D is an autoimmune disease in which an immune response is aberrantly directed against the insulin-producing beta cells located in the pancreatic islets of Langerhans. Like many autoimmune diseases, genetic factors contribute to but are not sufficient for the development of T1D. Environmental factors also appear to play a role, although specific environmental triggers remain poorly understood. T1D has also been referred to as juvenile diabetes, as onset typically occurs during childhood or young adulthood. Its prevalence in the U.S. is rising. In 2011, 25.8 million people in the U.S., or 8.3% of the population, were living with T1D, resulting in a cost of approximately $245 billion annually (CDC, 2011).

Much of our understanding of the pathogenesis of T1D has come from the study of the non-obese diabetic (NOD) mouse. NOD mice are a genetically distinct inbred strain that spontaneously develop islet-directed autoimmunity similar to that seen in human T1D (Anderson and Bluestone). Physiologic beta cell remodeling at around 2 weeks of age causes a release of antigen that in NOD mice leads to priming of islet-reactive T cells in the draining pancreatic lymph node (PLN) (Turley et al., 2003). Once activated, these T cells drive disease by infiltrating the pancreatic islets and destroying the beta cells. This islet immune infiltration is also referred to as insulitis and can be

divided into multiple classifications. The early stage is referred to as peri-insulitis, in which immune cells congregate at the periphery of the islet. As disease progresses, the immune infiltrate advances across the islet to become full-blown insulitis. Finally, after beta cell destruction is complete, the lack of persistent antigen can lead to eventual clearance of the immune infiltrate. Notably, islet infiltration levels typically are not synchronized in all islets of a given animal. Rather, individual islets will exhibit varying levels of infiltration at any given time during disease progression. Diabetes onset occurs when sufficient beta cell mass has been destroyed such that animals become hyperglycemic, which can be detected by blood or urine glucose levels greater than 250 mg/dl.

Although T1D is a T cell driven autoimmune disease, a number of other immune cells contribute to disease pathogenesis. Dendritic cells (DCs) are critical disease mediators because they are the primary antigen-presenting cells (APCs) of the immune system, displaying antigen to cognate T cells and providing ancillary signals to promote either T cell tolerance or immunity. DCs are the only immune cells present in healthy islets and are among the first cells recruited in the early disease stages (Jansen et al., 1994; Shinomiya et al., 2000). DC depletion in pre-diabetic NOD mice leads to a clearance of islet infiltrates and a delay in disease that corresponds to the duration of DC depletion (Saxena et al., 2007). Genetic deletion of B cells, which are present in high numbers in infiltrated islets, renders NOD mice resistant to diabetes development (Serreze et al., 1996). Transfer of sera from diabetic NOD mice does not overcome this resistance; suggesting that autoantibodies are dispensable to disease development (Serreze et al., 1998). Furthermore, depletion of B cells with rituximab, an anti-CD20

antibody, in diabetic mice and even in human patients ameliorates disease (Hu et al., 2007; Pescovitz et al., 2009), indicating that in addition to DCs, B cells also function as essential APCs in T1D. Additional immune cells present within the islet infiltrate include NK cells, plasmacytoid DCs (pDCs), and macrophages.

Tregs in T1D

The key role of Tregs in the maintenance of immune tolerance lead many investigators to uncover defects in these cells in settings of autoimmunity (Tang and Bluestone, 2006). In T1D specifically, studies in human patients have examined both the number and function of Tregs present in peripheral blood. While most studies did not detect a defect in Treg numbers in T1D patients compared to healthy controls (Brusko et al., 2007; Brusko et al., 2005; Lindley et al., 2005; Putnam et al., 2005), the functional suppressive capacity of Tregs from T1D patients compared to healthy controls has been found to be reduced (Brusko et al., 2005; Lindley et al., 2005). Further work has shown that the reduced suppressive capacity of Tregs from T1D patients may be due to IL-2 signaling defects present in these cells (Long et al., 2010). Still other studies have demonstrated that effector T cells in T1D patients may be more resistant than effector T cells from healthy controls to Treg suppression (Lawson et al., 2008; Schneider et al., 2008).

These studies in human T1D patients all have the caveats of being *in vitro* studies of T cells from peripheral blood, which may or may not be representative of the setting in the target tissue. Indeed, studies in the NOD mouse have shown that while their

peripheral Treg number and function is relatively normal, the frequency and function of these cells in the target tissue declines over time with disease progression (Tang et al., 2008). Additional evidence pointing to a Treg defect in autoimmune diabetes comes from studies showing that *in vivo* induction (Bresson et al., 2006) or adoptive transfer (Tang et al., 2004; Tarbell et al., 2004b) of Tregs in NOD mice protects against disease development and can reverse disease in recent-onset animals.

While many treatments can prevent diabetes onset in NOD mice, ones like Treg therapy that can restore euglycemia after disease onset are much less common. However, multiple therapeutic approaches that have cured diabetes in NOD mice have failed to produce the same results when tested in humans. Ongoing studies described below will determine whether Tregs may break this mold. In the clinic, most patients are diagnosed at a time where the majority of the beta cell mass is already lost and euglycemia can no longer be independently maintained. The time following diagnosis is frequently followed by a "honeymoon" period where the patient still produces residual amounts of insulin as measured by detectable c-peptide levels in the blood. In the absence of beta cell replacement therapy, the honeymoon period and the pre-diabetic phase are when immune intervention strategies could potentially be the most effective.

Tregs for cellular therapy

The preclinical data demonstrating the power of Tregs to modulate immune responses has led to great interest in manipulating these cells for therapeutic benefit in a number of contexts. In the settings of autoimmunity and transplant rejection, where an

over-exuberant immune response causes damage to the host, it is believed that a boost in Tregs may provide protection. Two potential approaches can be envisioned to boost Tregs *in vivo*. The first would be treatments to induce, expand or in some other way favor endogenous Tregs in the patient. The second would be to infuse the patient with exogenous Tregs. Current efforts are pursuing both approaches.

In the realm of adoptive Treg therapy, the first completed phase I clinical trials tested the safety of polyclonal Tregs in the treatment of GVHD (Brunstein et al., 2011; Di Ianni et al., 2011; Trzonkowski et al., 2009). These studies employed Tregs isolated from third-party donors that were either infused directly after isolation (Di Ianni et al., 2011) or expanded *in vitro* prior to infusion (Brunstein et al.; Trzonkowski et al.). While the primary endpoint of safety was met in these studies, they also demonstrated some evidence of efficacy in hindering GVHD. In the setting of autoimmune disease, the first clinical trials with Tregs are being done in T1D. A group from Poland was the first to report on testing autologous *in vitro* expanded polyclonal Tregs in 10 children with recent onset T1D (Marek-Trzonkowska et al., 2012). No adverse safety effects were observed in this study, and Treg-treated subjects showed less dependency than controls on exogenous insulin throughout the 4-month post-infusion follow-up. At UCSF, a similar study in young adults with recent onset T1D is ongoing. This study is testing the safety of escalating doses of autologous *in vitro* expanded polyclonal Tregs, with patients at the highest doses receiving 2.6×10^9 Tregs. These patients will be followed to monitor safety and possible effects of Treg therapy on residual beta cell function.

While trials using polyclonal Tregs are an important first step, mouse studies have shown that antigen-specific Tregs may be necessary to achieve effective and specific

immune suppression. Trials currently under development will begin to explore the use of antigen-specific Tregs in humans. Of note, the ONE study is a multi-center 5 year project that is comparatively testing multiple cellular immune therapies to prevent rejection of kidney transplants. Each team collaborating in the study will test a different immunoregulatory cell treatment. The cells to be tested will include polyclonal Tregs as well as Tregs that have been *in vitro* expanded by stimulation with donor-derived APCs, which leads to an outgrowth of donor-specific Tregs.

In its current state, Treg isolation and expansion for clinical use is a cumbersome and expensive process that can only be carried out by experienced groups with specialized clinical grade reagents and facilities. As most trials are currently testing the use of autologous cells, the process must be carried out for each individual patient. Even if ongoing trials demonstrate clinical benefit from Treg therapy, technological advancements to overcome production challenges will be necessary in order for such therapies to achieve widespread clinical use.

As an alternative means of achieving tolerance through Tregs, other groups are pursuing means to boost endogenous patient Tregs *in vivo*. Some of these methods, such as tolerogenic DC therapy, still rely on *in vitro* manipulated cells and therefore face some of the same challenges as Treg cell therapy. Others however aim to utilize small molecules or biologics to boost endogenous Tregs. Such approaches come with their own challenges. The *in vivo* balance between immunity and tolerance is very delicate. One recent study based on promising pre-clinical data treated T1D patients with IL-2 and rapamycin in an effort to boost Tregs but ended up with deleterious effects due to an unintended boost of NK cells (Long et al., 2012). Such an example illustrates the

difficulty of trying to manipulate an ongoing *in vivo* immune response and demonstrates the need to maximize our understanding of disease pathogenesis and immune function in order to make well-informed decisions on the best therapeutic approaches to test in patients.

Which, if any, of these approaches will be successful in suppressing aberrant immune responses in humans remains to be determined. Results from these initial trials will likely determine the course for future therapeutic use of Tregs. At the same time, ongoing studies in pre-clinical models such as those described in this dissertation will help to further our understanding of Treg biology and immune tolerance to lay the foundations for future clinical advancements.

CHAPTER II: REGULATORY T CELLS EXERT MULTI-LEVEL SUPPRESSION OF CD8$^+$ T CELLS IN THE TARGET TISSUE IN AUTOIMMUNE DIABETES

Abstract

Therapeutic regulatory T cells (Tregs) can prevent and even reverse autoimmune pathology in mouse models. We aimed to determine the means by which therapeutic Tregs control pre-established inflammation using a mouse model of autoimmune diabetes. Islet antigen-specific Tregs infiltrated inflamed islets soon after infusion into pre-diabetic mice, which was quickly followed by a selective reduction of mRNA transcripts associated with cytotoxic T lymphocytes in the islets. This change was partially due to decreased CD8$^+$ T cell accumulation in the tissue. CD8$^+$ T cells that remained in the islets after Treg treatment were able to dynamically engage dendritic cells in a manner similar to that found in untreated mice, consistent with persistent islet dendritic cell activation following Treg treatment. Nonetheless, Treg treatment abrogated IFNγ production by CD8$^+$ and CD4$^+$ islet T cells. This suppression took place at the protein level with minimal effect on IFNγ mRNA. We found that maintaining IFNγ protein expression was dependent on activation of the mTOR pathway, which was suppressed in islet CD8$^+$ T cells *in vivo* following Treg treatment. Altogether, these results indicate that Tregs restrain CD8$^+$ T cells in inflamed tissue by limiting their accumulation and suppressing their effector program.

Introduction

Regulatory T cells (Tregs) are critical for the maintenance of immune homeostasis under steady-state conditions and are also capable of suppressing ongoing immune responses *in vivo*. Multiple molecular mechanisms of Treg suppression have been described. These include but are not limited to: expression of suppressive molecules such as CTLA-4, IL-10, TGF-β and IL-35, generation of adenosine by CD39 and CD73, deprivation of IL-2 from other T cells, and killing of targets cells via perforin and granzyme dependent mechanisms (Tang and Bluestone, 2008; Yamaguchi et al., 2011). The specific deployment for each of these mechanisms is likely dependent on disease setting and timing.

The impact of Tregs on target cells have also been investigated. Treg suppression of dendritic cell (DC) activation has been shown to be important in the maintenance of immune homeostasis and prevention of self-reactive T cell priming in the steady-state (Kim et al., 2007). This function depends on Treg expression of CTLA-4 (Onishi et al., 2008; Wing et al., 2008). While most studies focused on the effect of Tregs on CD4$^+$ conventional T cells, some analyzed their impact on CD8$^+$ T cells. Tregs have been shown to suppress CD8$^+$ T cell activation *in vitro* (Piccirillo and Shevach, 2001) and in the context of immunization *in vivo* (McNally et al., 2011). In a tumor setting, Tregs do not interfere with differentiation of CD8$^+$ T cells to cytotoxic T lymphocytes (CTL), but inhibit CTL killing of target cells in lymph nodes (Mempel et al., 2006). Recent work has also highlighted NK cells as targets of Treg suppression in the steady-state (Gasteiger et al., 2013a; Gasteiger et al., 2013b) by reducing IL-2 availability.

In an ongoing immune response when T cell priming is established, such as in the setting of chronic autoimmune diseases, Tregs must act on pre-activated cells to mitigate further damage in the target tissues. In this context, Tregs were found to suppress established inflammation in the intestine mediated by CD4^{+} T cells (Collison et al., 2007; Pandiyan et al., 2007). These studies have shown that Tregs can suppress further T cell proliferation and activation, as well as effector T cell survival, migration into the target tissue or their function. The impact of Treg suppression on other cell types in the tissue such as DCs and CD8^{+} T cells, which are often major contributors to an autoimmune response driven by polyclonal T cells, has not been thoroughly investigated. In the situation of ongoing autoimmunity, Treg suppression of CD8^{+} T cells and the actions of Tregs on DCs to limit T cells responses warrants further investigation.

The non-obese diabetic (NOD) mouse is a widely used model of type 1 diabetes (T1D) in which autoimmune infiltrates spontaneously develop in the pancreatic islets of Langerhans leading to beta cell destruction. In this model, both CD8^{+} and CD4^{+} T cells are essential drivers of pathogenesis, and are accompanied in the islet immune infiltrate by multiple other cell types including DCs, NK cells and B cells (Anderson and Bluestone, 2005a). Cytokines and cytotoxic mediators produced by CD4^{+} and CD8^{+} T cells directly and indirectly kill beta cells. CD8^{+} T cell killing of beta cells leads to more beta cell antigen shedding and amplification of the autoimmune response early after the initiation of the pathology (Wang, 1996). DCs are massively recruited to inflamed islets and further amplify the autoimmune response, thereby increasing antigen presentation to autoreactive T cells (Melli et al., 2009). In addition, CD8^{+} effectors can accumulate massively in the islets at later stages of the disease shortly before onset of frank diabetes

(Santamaria, 2003). Moreover, CD8$^+$ T cells are the most abundant immune cell among the islet infiltrates of recent onset T1D patients (Willcox et al., 2009), and analysis of samples from the JDRF Network for Pancreatic Organ donors with Diabetes (nPOD) has demonstrated the islet autoreactivity of these CD8$^+$ T cells in both recent onset and longstanding T1D patients (Coppieters et al., 2012). Altogether, these data highlight the important role of CD8$^+$ T cells in T1D pathogenesis and suggest that regulating these cells might be critical to suppressing ongoing tissue destruction.

Tregs from TCR transgenic NOD.BDC2.5 mice are islet-antigen specific and are 100% effective at preventing diabetes in pre-diabetic NOD mice (Tang et al., 2004; Tarbell et al., 2004a). This treatment is also effective when given to mice with recent diabetes onset with severe insulitis, suggesting that Tregs must be able to halt ongoing autoimmune responses in the inflamed tissue. In this study, we sought to elucidate the cellular targets of therapeutic BDC2.5 Tregs in the suppression of an ongoing immune response in the pancreatic islets. We took advantage of the strain of NOD mice deficient in the costimulatory molecule CD28 (NOD.CD28$^{-/-}$). These mice develop rapid, synchronous, and more aggressive diabetes with 100% penetrance, primarily due to their deficiency in Tregs (Salomon et al., 2000). BDC2.5 Treg treatment of NOD.CD28$^{-/-}$ mice at a time when insulitis is well established is completely protective against diabetes development (Tang et al., 2004). The stark contrast in disease outcomes between Treg-treated and untreated NOD.CD28$^{-/-}$ mice offers an ideal *in vivo* model in which to study Treg function in controlling a multifaceted autoimmune disease mediated by polyclonal T cells. By probing the alterations in the islet immune infiltrate within the first week

following Treg treatment, we have identified CD8^{+} T cells as early targets of Treg-mediated immune suppression at the site of inflammation.

Materials and Methods

Mice

NOD.CD28^{-/-}, NOD.CD11c-YFP.CD28^{-/-}, NOD.BDC2.5.Thy1.1 TCR transgenic, NOD.uGFP.BDC2.5.Thy1.1 TCR transgenic, and NOD.8.3.Thy1.1 TCR transgenic mice were housed and bred under specific pathogen-free conditions at the University of California Animal Barrier Facility. The Institutional Animal Care and Use Committee of University of California approved all experiments.

Islet isolation

Pancreas was perfused with 3 ml of HBSS (Hyclone) containing 0.8 mg/ml collagenase P (Roche) via cannulated common bile duct (Lenschow et al., 1995). The distended pancreas was excised, incubated at 37°C for 16 min, and gently tapped to release islets. Pancreatic islets were further purified by Histopaque-1119 (Sigma-Aldrich) density-gradient centrifugation and handpicked under a dissecting microscope.

qRT-PCR

For whole islet analysis, handpicked islets were lysed in TRIzol (Invitrogen). For analysis of sorted islet cell populations, cells were FACS sorted into TRIzol LS (Invitrogen). RNA was extracted using RNeasy Micro columns (QIAGEN). Reverse

transcription was done using SuperScript III (Invitrogen). qRT-PCR used SYBR Green

Mastermix (SABiosciences) on the Bio-Rad CFX 96 platform. For whole islet

experiments, a RT^2 Profiler Custom PCR Array (SABiosciences) was used to

simultaneously examine transcript levels of 86 genes selected for their relevance to T1D,

along with 4 housekeeping genes and controls for genomic DNA contamination, RNA

quality and general PCR performance (gene list can be found in **Table 1**). For assaying

transcripts of individual genes in sorted islet cells, individual qPCR primers were used

(SABiosciences).

Fluorescent confocal microscopy

Pancreata were frozen in Tissue-Tek O.C.T. Compound (Sakura Finetek). 8-um sections

were stained overnight with Alexa 488-labeled anti-phospho-S6 ribosomal protein (2F9;

Cell Signaling Technology) and Alexa 647-labeled anti-CD8 (YTS169; UCSF

Monoclonal Antibody Core). Nuclei were visualized with DAPI. Images were acquired

on a Leica SP5 Confocal microscope using a 63x water immersion objective with the aid

of the Leica Application Suite Advanced Fluorescence Lite software. Post-acquisition

analyses and visualization were performed using Leica Application Suite Advanced

Fluorescence Lite software and Imaris software (Bitplane AG). Enumerating the number

of CD8$^+$ T cells per islet and the percentages that were pS6$^+$ was manually done in a

blinded manner by an independent party.

Two-photon microscopy

Handpicked islets were stained in 5 ug/ml Hoechst for 15 min at room temperature and embedded in RPMI medium containing 0.5% low melting point agarose (Invitrogen) on a plastic coverslip. The embedded islets were placed in a flow chamber perfused with RPMI medium without phenol red saturated with 95% O_2/5% CO_2. Temperature within the chamber was maintained between 36 and 37°C during the entire imaging period. Images were acquired on a custom-built 4 PMT detector video-rate two-photon microscope using a water immersion 20x/0.95 NA objective with the aid of Micromanager software. For time-lapse image acquisition, z-stacks with up to 40 xy planes with 5 um spacing were acquired every 30 or 60 s for 20-60 min. Data were visualized and analyzed using Imaris software (Bitplane AG).

Flow cytometry

Handpicked islets were dissociated into single cells by incubating in Gibco Cell Dissociation Buffer (Invitrogen) for 30 min in a 37°C water bath, followed by mechanical disruption by pipetting up and down. Cells were then filtered and washed before staining. LN cells were made into a single cell suspension by mechanical disruption. When analyzing DCs, LNs were digested with collagenase D (Roche). The following antibodies were used to stain the cells: anti-CD4-PE, anti-CD8-Pacific orange, anti-CD45-APC-Cy-7, anti-Thy1.1-PerCP, anti-Thy1.2-AL700, anti-B220-Pacific blue, anti-CD11c-PE-Cy7, anti-Ki67-FITC, anti-Bcl2-PE, anti-IAg7-AL700 anti-CD40-PE, anti-CD80-biotin, and anti-CD86-APC. For intracellular cytokine staining, cells were fixed with 4% PFA for 5 min at room temperature following surface staining. Fixed cells were permeabilized in 0.1% saponin and stained with anti-IFNγ-PE-Cy7 (XMG1.2;

eBioscience). Analyses were performed on a LSRII or Fortessa flow cytometer (BD Biosciences) with FACSDiva analysis software (BD Biosciences).

Phosphoflow

Dissociated islet cells were incubated overnight at 37°C in 0.15 ml of RPMI 1640 + 10% FCS in a 96 well U-bottom plate at 2-3 x 10^5 cells per well. Following 5 min incubation with fixable viability dye eFluor 780 (eBioscience), cells were fixed in Lyse/Fix buffer (BD Biosciences) at 37° for 10 min. Permeabilization was done by a 30 min 4° incubation in Perm buffer III (BD Biosciences), followed by concurrent staining of surface markers and intracellular phospho-ribosomal protein S6-Alexa488 (2F9; Cell Signaling Technology).

In vivo Brefeldin A treatment for intracellular cytokine staining

In vivo BFA treatment was adapted from a previously published method (Liu and Whitton, 2005). Mice were retro-orbitally injected with 250 ug BFA (Sigma-Aldrich) 4 h prior to sacrifice. Islet isolation was carried out as above, with the addition of 10 ug/ml BFA to the media during pancreas digestion, density-gradient centrifugation, and handpicking. Handpicked islets were cultured at 37° for an additional 2 h in RPMI with 10 ug/ml BFA. Islet dissociation was also carried out in the presence of 10 ug/ml BFA and staining proceeded as described above.

Cell transfers

For BDC2.5 Treg treatments, FACS-purified $CD4^+CD62L^{high}CD25^+$ Tregs from lymph nodes of NOD.BDC2.5.Thy1.1 TCR transgenic mice were expanded with anti-CD3/CD28 coupled Dynabeads (Invitrogen) for 10 days in the presence of 2000 IU/ml rhIL-2 in DMEM and 10% FCS as previously described (Tang et al., 2004). Purity of the culture was determined at the end of the expansion by analyzing an aliquot for Foxp3 expression using flow cytometry. BDC2.5 Treg-treated mice were i.p. injected with 10^6 of the *ex vivo* expanded BDC2.5 Tregs at 5 to 7 weeks of age. For two-photon imaging experiments at 18 h – 3 days post-Treg transfer, 3-5 x 10^6 BDC2.5 Tregs were labeled with CMTMR (Invitrogen) and i.v. injected. For two-photon imaging experiments at day 7 post-Treg transfer, NOD.uGFP.BDC2.5 mice were used as the source of Tregs, with isolation and expansion as above, followed by injection of 10^6 Tregs.

For 8.3 $CD8^+$ T cell transfers, $CD8^+$ T cells were negatively selected from spleens of NOD.8.3.Thy1.1 TCR transgenic mice. Unwanted cells were labeled with biotinylated antibodies (all from the UCSF monoclonal antibody core) - CD19 (6D3), CD11b (M1/70), and CD4 (GK1.5) – and depleted using Dynabeads Biotin Binder (Invitrogen). Enriched $CD8^+$ T cells were labeled with CMTMR or CFSE (Invitrogen) and i.v. injected, 8-10 x 10^6 CD8 T cells for two-photon experiments, and 1 x 10^6 $CD8^+$ T cells for proliferation and cytokine experiments. For BDC2.5 $CD4^+CD25^-$ transfers, $CD4^+$ T cells were negatively selected from spleens of NOD.BDC2.5.Thy1.1 TCR transgenic mice in the same manner as for $CD8^+$ selection. Biotinylated antibodies used were CD19 (6D3), CD11b (M1/70), CD8 (53-6.7; eBioscience), and CD25 (PC.61; UCSF monoclonal antibody core). Enriched $CD4^+$ T cells were labeled with CFSE and i.v. injected at 10^6 $CD4^+$ T cells per mouse for proliferation and cytokine experiments. For

intracellular cytokine and proliferation experiments, bead-enriched cells were further

negatively sorted by FACS to high purity.

ELISA

Dissociated islet cells were incubated overnight at 37°C in 0.15 ml of RPMI 1640 + 10%

FCS in a 96 well U-bottom plate at 2-3 x 10^5 cells per well. 0.1 ml of undiluted

supernatant was used to measure IFNγ concentrations using a standard sandwich ELISA.

Briefly, plates were coated with capture anti-IFNγ antibody (R4-6A2; BD Pharmingen) at

3 ug/ml. Biotin-conjugated anti-IFNγ (XMG1.2; BD Pharmingen) was used at 0.3 ug/ml

as the detecting antibody.

Statistical analysis

Statistical analyses were performed with the aid of Prism software (GraphPad) using the

tests indicated.

Results

Tregs engage islet DCs in dynamic interactions

 To understand how Tregs may exert their suppressive function at the site of

inflammation in the pancreatic islets, we analyzed their dynamics and their interactions

with islet-resident DCs in real-time by time-lapse two-photon imaging of isolated, intact

islets. Fluorescently labeled BDC2.5 Tregs were transferred to NOD.CD11c-YFP.CD28$^-$

$^{/-}$ mice, in which CD11c$^+$ DCs can be visualized by their expression of YFP. Islets were

isolated for imaging at 18 hours and 2, 3 and 7 days after transfer. For imaging during

the first three days after transfer, a red fluorescent vital dye, CMTMR, was used to label

Tregs. As BDC2.5 Tregs proliferated in the islets (data not shown), CMTMR was diluted

out over the course of multiple cell divisions. In order to visualize Tregs at day 7 post-

transfer, Tregs from NOD.uGFP.BDC2.5 mice, which express GFP under the control of

the ubiquitin promoter, were used for imaging at this time-point. Regardless of the time

of imaging, transferred Tregs were found within the islets and were seen to make

dynamic interactions with islet DCs, which formed a continuous network in inflamed

islets (**Fig. 1**). While some Tregs formed stable interactions with islet DCs that persisted

for the entire 20-30 minute imaging period, it was more common to see a Treg form

multiple short contacts with one or more DCs. Overall, average Treg velocity was

around 5-6 um/min and most cells were relatively confined to a general area – often

around DCs – as measured by their relatively low track displacement to track length

ratios (**Fig. 1 B and C**). Taken together, this behavior closely resembles what we have

previously described in the draining pancreatic lymph node (PLN) as "swarming"

behavior (Tang et al., 2006). Overall, these imaging studies demonstrated that Tregs

rapidly home to the islets – within 18 hours post-transfer. Upon islet entry, Tregs neither

move freely throughout the tissue, nor do the majority fully arrest on DCs; rather, short,

repeated contacts between Tregs and DCs are the most commonly observed behaviors at

all time-points examined.

Tregs down-regulate a CTL signature in the islets

While BDC2.5 Treg treatment completely protects against progression to diabetes

in pre-diabetic NOD.CD28$^{-/-}$ mice, it does not result in a clearance of insulitis, even at

multiple months post-treatment. Similarly, NOD.BDC2.5 mice themselves contain large

immune infiltrates in the islets, the destructive potential of which are held in check by the

Tregs acting particularly in the islets (Chen et al., 2005; Feuerer et al., 2009). To

examine how therapeutic Tregs gain control over the immune infiltrate, we developed a

96-well qRT-PCR array that contained genes relevant to the immunopathology of T1D.

The types of genes included were: markers of specific immune cell populations, markers

of beta cell function, chemokines and their receptors, costimulatory molecules, cytokines,

immune effector molecules, adhesion molecules, housekeeping genes, and internal PCR

controls (See **Table 1** for the full list of genes). We analyzed whole islet mRNA from

NOD.CD28$^{-/-}$ mice at the time of BDC2.5 Treg treatment and at 3 and 7 days following

Treg treatment, along with islet mRNA from age-matched untreated littermate controls.

Untreated mice showed a progressive decline of insulin expression, demonstrating

advancing beta cell destruction in these mice (**Fig. 2 A**). In contrast, mRNA for both

insulin 1 and insulin 2 genes steadily increased in Treg-treated mice when compared to

that found at baseline, indicating a decrease in beta cell stress and not only preservation

but also restoration of insulin production.

When comparing islets 3 days post-Treg treatment to untreated age-matched

controls, the largest changes were a downregulation of granzyme A and granzyme B

mRNA (**Fig. 2 B**). At 7 days post-Treg transfer, further downregulation of these

cytotoxic effector molecules was observed. Additional genes down-regulated three-fold

or more in Treg-treated mice at this time-point included the chemokines Cxcl9 and Xcl1,

and IFNγ (**Fig. 2 C**). NK cells express granzymes and IFNγ, and have been implicated to

be a primary Treg target in BDC2.5 TCR transgenic mice (Feuerer et al., 2009).

Consistent with this previous report, we found that the NK cell marker Klrd1 was reduced 4.6-fold 7 days after Treg treatment (**Fig. 2 C**). However, the expression level of this marker was low even in control samples (average Ct value of 31.2 +/- 1.2), suggesting low prevalence of this cell subset in the inflamed islets. Flow cytometric analysis of inflamed NOD.CD28$^{-/-}$ islets showed that NK cells made up on average approximately 2% of the total immune cell infiltrate. In contrast, CD8$^+$ T cells represented an average of about 10% of the immune infiltrate. CD8α was reduced 5.3-fold 7 days after Treg treatment (**Fig. 2 C**), while markers for other major cell populations remained relatively unchanged (reductions of 1.5-fold for CD11c and 2.2-fold for CD4). Altogether these changes implicated cytotoxic CD8$^+$ T cells as the immediate and specific targets of Treg suppression in inflamed islets.

Tregs reduce CD8$^+$ T cell accumulation in the islets

The decreased CTL transcriptional signature observed in Treg-treated islets, especially the down-regulation of the cell surface marker CD8α suggested that there may be reduced numbers of CD8$^+$ T cells within the islets following Treg treatment. To test this, intra-islet CD8$^+$ T cells were enumerated after immunofluorescence staining of CD8 in pancreas sections from NOD.CD28$^{-/-}$ mice at 7 days post-Treg treatment and in age-matched controls. Significantly fewer CD8$^+$ T cells per islet were observed in sections from Treg-treated mice than in controls (**Fig. 3 A**).

This decrease in CD8$^+$ T cells could arise from decreased recruitment from the circulation, retention in the tissue, *in situ* proliferation, or survival in the islets. Analysis of the cell cycle marker Ki67 by flow cytometry showed no differences in expression

between islet CD8$^+$ T cells of control mice and mice 7 days post-Treg treatment (**Fig. 3 B**). Similarly, islet CD8$^+$ T cell expression of the survival marker Bcl2 was also unchanged at this time point (**Fig. 3 C**). Together, these data indicated that a reduction in local proliferation or survival did not contribute to the reduced numbers of islet CD8$^+$ T cells.

Since peripheral CD8$^+$ T cells in NOD mice and in other models of inflammation express the chemokine receptor Cxcr3 (data not shown and (Hu et al., 2011)), and one of its ligands, Cxcl9, was reduced in the islets after Treg treatment, we assessed if Treg treatment inhibited CD8$^+$ T cell trafficking to the islets. To do this, we examined the accumulation of adoptively transferred islet-reactive CD8$^+$ T cells in inflamed islets of NOD.CD28$^{-/-}$ mice that had either been treated or not with Tregs 7 days prior. CD8$^+$ T cells from NOD.8.3 mice, which express a transgenic TCR that is specific for the β cell antigen IGRP (Verdaguer et al., 1997), were negatively selected using magnetic bead enrichment and stained with CMTMR before adoptive transfer into NOD.CD28$^{-/-}$ recipients. Islets from the recipient mice were isolated 18 hours later and examined for the presence of transferred 8.3 T cells using two-photon microscopy. Significantly fewer 8.3 T cells were seen within the islets of Treg-treated mice than in the islets of control mice (**Fig. 3 D**). Together, these data suggest that the reduction in islet CD8$^+$ T cells observed histologically and by qPCR profiling of the islets was due at least in part to reduced recruitment and/or decreased retention of the cells following their arrival in the tissue.

Phenotypic islet DC changes following Treg treatment do not inhibit islet T cell-DC interactions

While Treg treatment reduced total islet $CD8^+$ T cell numbers, large numbers persisted, along with the rest of the islet immune infiltrate. Additionally, Treg suppression of $CD8^+$ T cell trafficking to the islets was incomplete, with a considerable number of cells continuing to enter the islets. This indicates that in addition to reducing the recruitment of new effector T cells to the islets, Tregs must also suppress the existing CD8 effectors. DCs are essential for sustaining inflammation in the islets (Nikolic et al., 2005; Saxena et al., 2007). We have previously shown that islet infiltration by T cells leads to massive recruitment of DCs and increases intra-islet DC CD80 and CD40 expression as an amplification loop of the autoimmune response (Melli et al., 2009). Other studies have implicated DCs as targets of Treg suppression (Onishi et al., 2008; Wing et al., 2008). In particular, Sakaguchi and colleagues have shown in a setting of *in vitro* activation that Treg-DC interactions reduce expression of the costimulatory molecules CD80 and CD86 on DCs (Onishi et al., 2008). Therefore, we tested the hypothesis that Tregs suppress $CD8^+$ T cells indirectly by suppression of DCs.

Using flow cytometry, we profiled expression of MHC class II and the costimulatory molecules CD80, CD86, and CD40 on islet DCs from NOD.CD28$^{-/-}$ mice at 7 days post-Treg treatment and in age-matched untreated littermates. Following BDC2.5 Treg treatment, no changes were observed in islet DC expression of MHC class II or CD80 (**Fig. 4 A**). In contrast, expression of CD86 and CD40 decreased in the islet DCs of mice treated with Tregs (**Fig. 4 A**); however, despite these decreases, expression levels of these molecules on Treg-treated islet DCs remained as high as or higher than the

levels observed on DCs in the draining PLN, demonstrating attenuation rather than a total loss of expression. In an attempt to determine the stimulatory capacity of islet DCs following Treg treatment, we employed an *ex vivo* culture assay. Islet DCs were isolated from NOD.CD28$^{-/-}$ mice at 7 days post-Treg treatment or from untreated littermates and placed in an *ex vivo* co-culture with 8.3 CD8$^+$ T cells and BDC2.5 CD4$^+$CD25$^-$ T cells without addition of exogenous antigens. At the end of the 4 day culture, we found that regardless of Treg treatment, islet DCs were effective at stimulating CD8$^+$ and CD4$^+$ T cell proliferation and IFNγ production, (**Fig. 4 B** and **C**), suggesting that they do not have defects in processing and presenting islet antigens and provide other ancillary signals to activate T cells.

This *ex vivo* approach has the caveat that DCs can be altered and mature upon isolation from the tissue (Schlecht et al., 2006); thus, the lack of difference in their function may not be indicative of a lack of differences *in vivo*. Therefore, we next determined if Tregs altered the ability of DCs to engage T cells in intact explanted islets without disrupting their three-dimensional structures and immediate tissue contacts. We performed time-lapse imaging of isolated islets from Treg-treated and control mice using two-photon microscopy. For these imaging experiments, CMTMR-labeled CD8$^+$ T cells from NOD.8.3 TCR transgenic mice were adoptively transferred into NOD.CD11c-YFP.CD28$^{-/-}$ mice that had been either treated or not 7 days prior with Tregs from NOD.uGFP.BDC2.5 mice. Islets were isolated for imaging the day after 8.3 T cell transfer. 8.3 CD8$^+$ T cells actively engaged DCs in both the presence and absence of BDC2.5 Tregs (**Fig. 5 A**). Quantification of 8.3 T cell dynamics showed relatively slow and similar velocities of 8.3 T cells in the presence and absence of BDC2.5 Tregs (**Fig. 5**

B). Additionally, we observed that CD8$^+$ T cells were significantly more confined in the presence of BDC2.5 Tregs (**Fig. 5 C**); further suggesting that Tregs did not disrupt T cell-DC interactions in the inflamed islets.

Tregs suppress islet T cell effector function

We next determined the functional impacts of Treg treatment on both newly recruited and pre-existing islet effector T cells. To examine whether Treg treatment inhibited the activation of newly recruited islet-reactive T cells within the islets, we FACS purified congenically marked CD8$^+$ T cells from NOD.8.3 mice and CD4$^+$CD25$^-$ conventional T cells from NOD.BDC2.5 mice, labeled the cells with CFSE, and transferred one million of each cell type i.v. into NOD.CD28$^{-/-}$ mice that had been treated with BDC2.5 Tregs 3 days prior. Mice were sacrificed 4 days later to assess the proliferation and cytokine production of the transferred T cells.

In agreement with our previous findings (Tang et al., 2006), Treg treatment inhibited proliferation of transferred T cells in the PLN (**Fig. 6 A**). By day 4 post-transfer, the majority of the transferred cells in control PLNs had completely diluted out their CFSE. However in PLNs of Treg-treated mice, 8.3 CD8$^+$ T cells were proliferating more slowly, as indicated by their incomplete CFSE dilution, and a significant percentage of BDC2.5 CD4$^+$ T cells had not gone into cycle at all. In contrast to the PLN, and in agreement with the lack of a Treg effect on islet T cell Ki67 expression (**Fig. 3 B**) or on islet T cell-DC dynamics (**Fig. 5**), transferred T cells in the islet tissue proliferated extensively, regardless of the presence or absence of BDC2.5 Tregs (**Fig. 6 A**). BDC2.5 T conventional cells (Tconv) showed no differences in proliferation in the presence of

BDC2.5 Tregs, while for 8.3 T cells, a moderate but significant attenuation of proliferation was observed. Overall though, this inhibition in the tissue was slight when compared to that observed in the draining lymph nodes. These results suggest that while the primary impact of Tregs in the lymph node is the suppression of T cell clonal expansion and priming, the effect of Treg therapy on T cells at the site of inflammation appears to be distinct.

Seeing that T cell proliferation in the islets remained generally unimpeded in the presence of Tregs, both by Ki67 staining of endogenous T cells and by CFSE dilution of transferred T cells, we next sought to examine the effects of Treg treatment on effector function of islet T cells. To do this, we measured islet T cell production of IFNγ in response to physiological *in vivo* antigen presentation. We adapted a previously described *in vivo* Brefeldin A (BFA) approach (Liu and Whitton, 2005), where animals were injected with BFA 4 hours before sacrifice. By assaying islet T cell IFNγ production directly *ex vivo* in this manner, we observed a near total inhibition of IFNγ production by both transferred 8.3 and BDC2.5 T cells in Treg-treated mice, while transferred T cells in islets of untreated littermate controls made considerable amounts of the protein (**Fig. 6 B**). For endogenous islet T cells, both CD4$^+$ and CD8$^+$, the suppression of IFNγ in Treg-treated mice compared to controls was also significant (**Fig. 6 C**).

The lack of IFNγ seen in endogenous islet T cells of Treg-treated mice using the *in vivo* BFA method indicated that the cells were not actively producing IFNγ within the islets. However, qPCR analysis of sorted CD8$^+$ and CD4$^+$ T cells from Treg-treated islets showed that these cells still expressed levels of IFNγ mRNA equivalent to their control

counterparts (**Fig. 6 D**). Taken together, these islet T cells appear to be similar to anergic

cells described by others (Villarino et al., 2011), where cytokine mRNA but not protein is

expressed. These results indicated that Tregs can block effector T cell function at the

final stages, suppressing effector protein production in the persistent presence of mRNA.

Tregs suppress mTOR signaling in islet CD8$^+$ T cells that is critical for IFNγ production

The mTOR pathway plays a critical role in CD8$^+$ T cell effector versus memory

balance (Araki et al., 2009; Pearce et al., 2009; Rao et al., 2010) and in CD4$^+$ T helper

cell differentiation (Delgoffe et al., 2009; Delgoffe et al., 2011). This pathway controls

multiple metabolic cell processes, including aerobic glycolysis and protein translation

(Powell et al., 2012). Furthermore, recent work in CD4$^+$ T cells has demonstrated a

direct requirement of aerobic glycolysis for translation of IFNγ mRNA but not for cell

proliferation or survival (Chang et al., 2013). Knowing this and having seen Tregs

suppress at a similar level in our system, we examined the role of mTOR in our model.

To probe the importance of mTOR signaling for sustaining islet T cell effector function,

we used an *ex vivo* islet cell culture where we could directly inhibit mTOR signaling with

the addition of the pharmacological mTOR inhibitor rapamycin. Inflamed islets isolated

from NOD.CD28$^{-/-}$ mice were dissociated and cultured overnight in the presence or

absence of rapamycin. The following day, cells were stained for flow cytometric analysis

of phosphorylation of ribosomal S6 protein (pS6) as a readout of mTOR signaling.

Ribosomal S6 protein is involved in protein translation and is activated via

phosphorylation by S6 kinase, which is activated by mTOR (Powell et al., 2012). Flow

cytometric analysis of islet cells cultured overnight without any exogenous stimulation

revealed that islet CD8$^+$ T cells, and to a lesser extent, CD4$^+$ T cells, contained readily detectable levels of phosphorylated S6 (pS6) (**Fig. 7 A**). Addition of rapamycin to the culture strongly inhibited this pS6, indicating that S6 phosphorylation primarily occurs downstream of mTOR in this setting. To test whether mTOR signaling was required for T cell effector function, culture supernatants were collected at the time of cell harvest for analysis of IFNγ concentrations. Rapamycin treatment strongly suppressed IFNγ production by islet cells (**Fig. 7 B**), suggesting that mTOR signaling was required for sustaining IFNγ production by effector T cells in inflamed islets.

Lastly, we determined whether mTOR signaling in CD8$^+$ effector T cells was affected by BDC2.5 Treg treatment. To analyze mTOR activation in islet T cells *in situ*, we examined pS6 levels in the islets using confocal immunofluorescence microscopy. Pancreas sections from NOD.CD28$^{-/-}$ mice at 7 days post-Treg treatment were stained alongside pancreas sections from untreated littermates to examine pS6 levels. pS6$^+$ cells were relatively frequent in infiltrated islets of untreated mice, and a proportion of these cells co-stained for CD8 (**Fig. 7 C**). In agreement with the low frequency of pS6$^+$ CD4$^+$ T cells observed in our *ex vivo* islet culture assay, pS6$^+$ CD4$^+$ T cells were not readily detected by immunofluorescence (data not shown). The percentage of islet CD8$^+$ T cells expressing pS6 was significantly lower in Treg-treated mice than in controls (**Fig. 7 C**). Taken together, these data show that mTOR signaling is essential to sustaining IFNγ production by intra-islet effector T cells, and Treg treatment terminated the effector program by intercepting the mTOR pathway.

Discussion

In investigating the means by which Tregs halt an ongoing autoimmune response in the target tissue, we have found the effects of Tregs to be manifold. While Treg treatment did not lead to a clearance of islet immune infiltrates, we did observe a significant reduction in the numbers of islet CD8^{+} T cells. This decrease was due at least in part to reduced recruitment and/or retention of these cells in the islets, whereas proliferation of intra-islet CD8^{+} T cells was not altered. The cytokine-regulated pro-survival protein Bcl2 was unaltered by Treg treatment, but we cannot rule out impaired survival of CD8^{+} T cells in a non-Bcl2-related manner. In addition to this suppression of CD8^{+} T cell accumulation, Tregs also modulated islet-resident immune cells. Using two-photon microscopy, we observed that Tregs engaged islet DCs but did not disrupt the interactions of these antigen-presenting cells with CD8^{+} T cells. While islet effector T cells received sufficient stimulation to proliferate in the presence of Tregs, their production of IFNγ was abrogated. In islet CD8^{+} T cells, this suppression of IFNγ production was linked to a decrease in mTOR signaling.

A novelty of this study is the identification of CD8^{+} effector T cells as a target of Treg suppression *in vivo* in a spontaneous autoimmune disease mediated by polyclonal T cells. Recent work by others has shown the importance of Treg suppression of immune cells other than CD4^{+} T cells, such as NK cells (Gasteiger et al., 2013a; Gasteiger et al., 2013b; Sitrin et al., 2013). In particular, studies examining NOD.BDC2.5.Foxp3-DTR mice have shown that Treg depletion leads to rapid diabetes due to activation of NK cells in the pancreas (Feuerer et al., 2009; Sitrin et al., 2013). As the BDC2.5 mice express a CD4^{+} TCR transgene, few CD8^{+} T cells are present in these mice. This difference may

account for the difference in the primary cytotoxic effectors (NK cells versus CD8^{+} T cells) in our two studies. Nonetheless, both studies emphasize the importance of Treg suppression of cytotoxic effectors in the control of an autoimmune response. In autoimmune diseases driven by a polyclonal T cell response, CD8^{+} T cells cause destruction both indirectly through the production of cytotoxic cytokines and directly via their recognition and killing of target cells expressing MHC Class I. Reigning in this destruction is paramount to preserving the target tissue. Recent work from our lab using a mouse model of islet transplant rejection has shown that CD8^{+} T cells are primary targets of therapeutic Tregs (K. Lee and Q. Tang, unpublished results). Altogether, these findings point to the importance of Treg suppression of CD8^{+} T cells in the context of *in vivo* disease mediated by polyclonal T cells.

When viewed in light of our previous work (Tang et al., 2006), this study demonstrates that Tregs suppress T cells in the draining lymph node and in the target tissue at different stages. While BDC2.5 Tregs in the PLN suppress the proliferation and differentiation of naïve T cells along with their interactions with LN DCs (Tang et al., 2006), we did not observe this suppression at the priming level in the islets. Rather, islet effector T cells engaged islet DCs and underwent proliferation, but were suppressed at the level of effector function following Treg treatment. These differences highlight the importance of location when considering mechanisms of Treg suppression.

In considering possible mechanisms of Treg suppression of effector T cells in the islets, we considered the three types of signals required to activate T cells and to sustain their effector function: TCR signaling, costimulation, and cytokine signaling. Knowing that DCs are a potent source of all of these signals, we investigated the effects of BDC2.5

Treg treatment on islet DCs. Work by others has suggested that Tregs may indirectly suppress T cell responses by down-regulating the costimulatory molecules CD80 and CD86 on DCs via CTLA-4 (Onishi et al., 2008; Wing et al., 2008). While we did not observe changes in islet DC expression of CD80 following Treg treatment, CD86 was moderately down-regulated. The main difference in our study from previous work is that we examined DCs from an inflamed tissue that were pre-activated at the time of Treg transfer. The experiments done by Sakaguchi and colleagues showed that *in vitro* co-culture of splenic DCs from a naïve mouse with Tregs suppressed the upregulation of CD80 and CD86 on DCs. In our model, the islet DCs are already expressing high levels of these molecules. It is possible that the short duration of the majority of the Treg-DC contacts observed in our two-photon imaging studies may not be prolonged enough to accomplish CTLA-4-mediated trans-endocytosis of CD80 or CD86 from the surface of DCs (Qureshi et al., 2011). If this trans-endocytosis is occurring, it is apparently not at high enough rates to dramatically effect expression levels on the DCs. Furthermore, the down-regulation of CD40 we observed has not appeared in previous studies. CD40 ligand (CD154) is primarily expressed on activated CD4$^+$ T cells, and CD40/CD40L interactions primarily serve to activate CD40-expressing DCs (Ma and Clark, 2009). While the possible effects of decreased CD154 signaling on differentiated effector T cells that could result from interactions with DCs with reduced CD40 expression should not be ruled out, we do not believe the modest decrease in islet DC CD40 expression to be primarily responsible for the observed decreases in islet T cell IFNγ production. Rather, the opposite may more likely be the case, where decreased T cell production of IFNγ at 7 days post-Treg results in reduced DC CD40 expression (Nguyen and Benveniste, 2000).

In examining how Tregs exert their suppressive effects on islet CD8^{+} T cells, we discovered that Tregs inhibit the metabolically important mTOR pathway in CD8^{+} T cells *in vivo*. The relationship between T cell metabolism and function has been extensively studied in recent years. For CD8^{+} T cells, mTOR signaling is well established as a critical regulator between effector and memory differentiation states; activation of the mTOR pathway has been shown to be critical in the generation of effector cells (Araki et al., 2009; Rao et al., 2010) while a decrease in mTOR signaling facilitates transition to a long-lived memory cell phenotype (Araki et al., 2009; Pearce et al., 2009). Here we have demonstrated that mTOR signaling is required to sustain the effector function of intra-islet effector T cells. We believe our study is the first to show that Tregs target this pathway as a means of suppressing CD8^{+} effector T cells. Since mTOR signaling was not readily detected in CD4^{+} T cells by our immunofluorescence approach, we cannot conclude that suppression of this pathway is also involved in the observed Treg suppression of CD4^{+} T cell IFNγ production. mTOR signaling through the TORC1 complex has been shown to be required for Th1 differentiation (Delgoffe et al., 2011); however, its requirement for maintaining effector function remains less well understood in CD4^{+} than in CD8^{+} T cells. Whether Tregs also target this pathway in differentiated islet CD4^{+} T cells to suppress their effector function remains to be determined.

mTOR can be activated by a number of external stimuli, including TCR ligation, costimulation, cytokine signaling, and nutrients such as amino acids. Based on our studies of islet DCs and their interactions with CD8^{+} T cells, we think it is unlikely that the disruption in mTOR signaling is due to inhibition of TCR or costimulatory signals. Inhibition of cytokine signaling, particularly IL-2 deprivation, has been shown by others

to be a mechanism by which Tregs can suppress CD4$^+$ T cells (Vignali et al., 2008), NK cells (Gasteiger et al., 2013b; Sitrin et al., 2013) and even CD8$^+$ T cells (McNally et al., 2011). IL-2, along with other common gamma chain cytokines, induces expression of the pro-survival protein Bcl2 (Akbar et al., 1996). The lack of Treg-mediated change in Bcl2 expression in islet CD8$^+$ T cells (**Fig. 2 C**) suggests that IL-2 deprivation may not be the mechanism at play in Treg suppression of effector T cell function. Future work in the lab will further investigate the means of mTOR inhibition in islet CD8$^+$ T cells following Treg treatment. As suppression of mTOR has been shown to favor differentiation of CD8$^+$ T cells into long-lived memory cells (Araki et al., 2009), it will be interesting to examine whether the islet CD8$^+$ T cells persisting after Treg treatment are skewed towards a long-lived memory phenotype. If so, this may represent a limitation of Treg therapy and help to explain the lack of complete islet infiltrate clearance in Treg-treated mice. Therapies that target memory cells, such as anti-IL-7 receptor-α (IL-7Rα) treatment have been shown to be effective in protecting against diabetes in NOD mice (Lee et al., 2012; Penaranda et al., 2012). Combining anti-IL-7Rα treatment with therapeutic Tregs could potentially have synergistic effects in reversing established T-cell dependent autoimmune disease.

Overall, this study has demonstrated that Tregs can function at multiple levels to inhibit *in vivo* disease progression. In addition to their ability to suppress T cell priming in the draining lymph node, Tregs can also inhibit the accumulation of effector cells in the target tissue. Perhaps most powerfully, Tregs in the tissue can suppress fully differentiated T cells at the functional level. This multi-functional capacity of Tregs is likely critical for their remarkable efficacy. Clinical efforts to target the immune system

in autoimmunity are increasingly revealing the likely need to take combinatorial approaches. As nature's original immune regulators, Tregs demonstrate the power of a multi-faceted approach. Continuing to further our understanding of how Tregs function *in vivo* may help identify critical targets for novel combinatory therapies and enhance our ability to harness the therapeutic potential of these cells.

Tables

Table 1. Custom 96-well qRT-PCR array gene list

Chemokines and chemokine receptors		Costimulatory molecules	Effector molecules
Ccl1	Cx3cl1	Cd40	Granzyme A
Ccl11	Cx3cr1	Cd40L	Granzyme B
Ccl12	Cxcl1	Cd80	
Ccl19	Cxcl10	Cd86	**Immune cell markers**
Ccl2	Cxcl11	Icos	CD11c
Ccl20	Cxcl12	OX40	CD3e
Ccl25	Cxcl13	OX40L	CD4
Ccl3	Cxcl16		CD45
Ccl4	Cxcl2	**Cytokines and cytokine receptors**	CD68
Ccl5	Cxcl9	Ifng	CD8a
Ccl7	Cxcr3	Il1a	Igsf6
Ccl8	Cxcr4	Il1b	Klrd1
Ccl9	Cxcr5	Il1rn	Foxp3
Ccr1	Cxcr6	Il1r1	Csf1r
Ccr10	Xcl1	Il1r2	Ly6c1
Ccr2	Xcr1	Il6	
Ccr3		Il10	**Beta cell function markers**
Ccr4		Il12b	Insulin I
Ccr5		Il15	Insulin II
Ccr6		Il16	Reg3a
Ccr7		Il-17f	Reg3b
Ccr8		Il27ra	Reg3g
Ccr9		Lta	
Ccrl2		Ltb	**Housekeeping genes**
		Ppbp	Hsp90ab1
		Tnf	Hprt1
			Gapdh
		Adhesion molecules	Actin-b

Icam1	
Madcam1	**PCR controls**
	Mouse Genomic DNA
Vcam1	Contamination
	Reverse Transcription Control - 2
Integrin-b2	wells
	Positive PCR Control - 3 wells

Figures

A

B

C
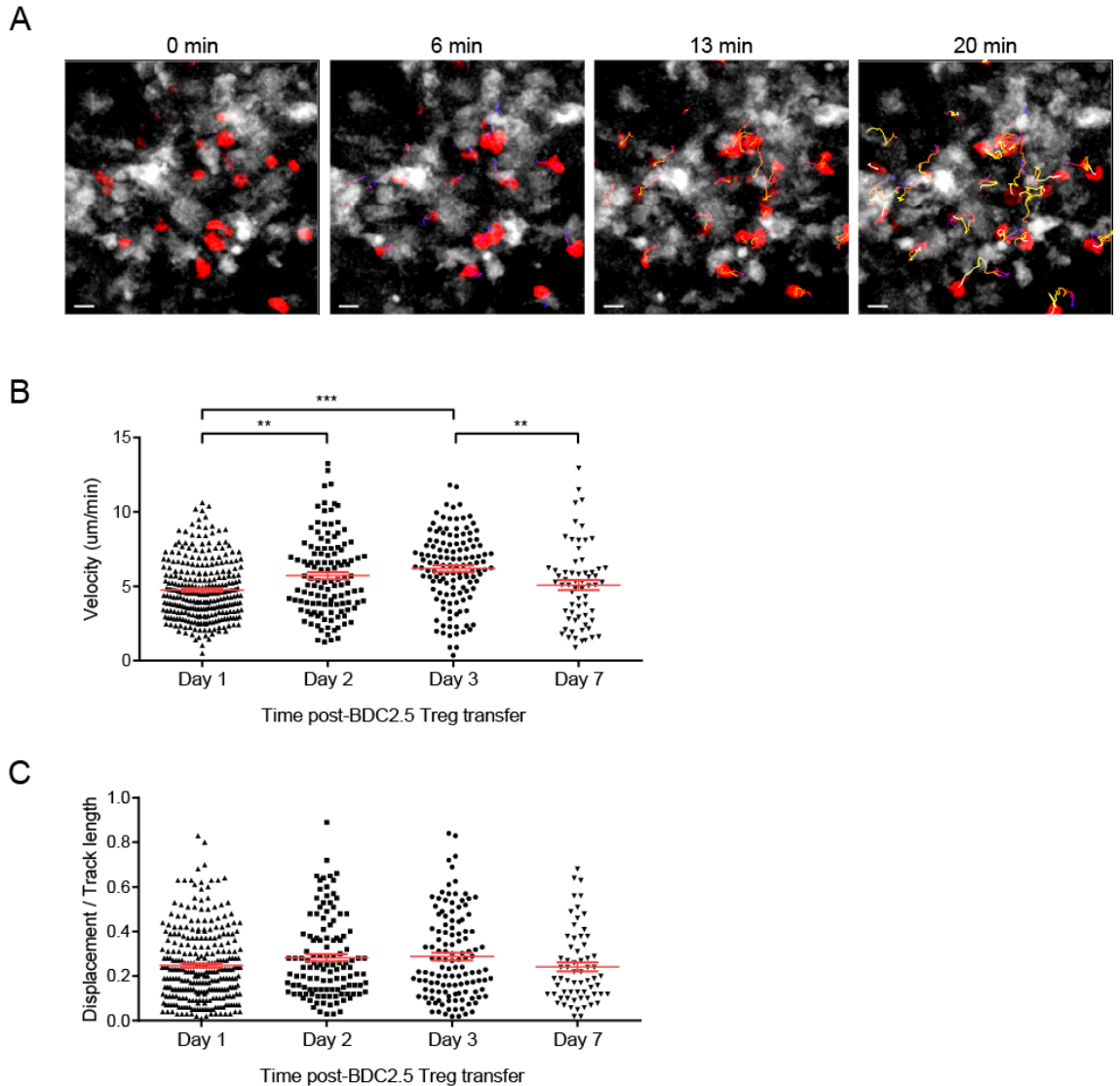
Figure 1. Tregs engage islet DCs in dynamic interactions.

(**A**) 3 x 10^6 CMTMR-labeled BDC2.5 Tregs were i.v. injected into a NOD.CD11c-

YFP.CD28$^{-/-}$ mouse. Islets were isolated 18 h later for imaging by two-photon

microscopy. Maximal projection time-lapse images from a representative islet show

BDC2.5 Tregs (red) crawling over islet CD11c$^+$ DCs (white). Track lines depict BDC2.5

Treg movements over the course of the 20 min imaging period and are color-coded

according to time (blue at the beginning of the imaging period to white at the end). Scale

bars represent 10 um. See Video 1 for full time-lapse. Graphs depict velocities (**B**) and

confinement ratios (**C**) of BDC2.5 Tregs at multiple time-points post-Treg transfer. Each

point represents a single cell, red bars represent mean + SEM. Data are from 3 to 13

islets per time-point imaged over 5 independent experiments. P values were determined

by Dunn's multiple comparison tests following Kruskal-Wallis test. **, $P < 0.01$; ***, P

< 0.001. No significant differences observed by Kruskal-Wallis test for C.
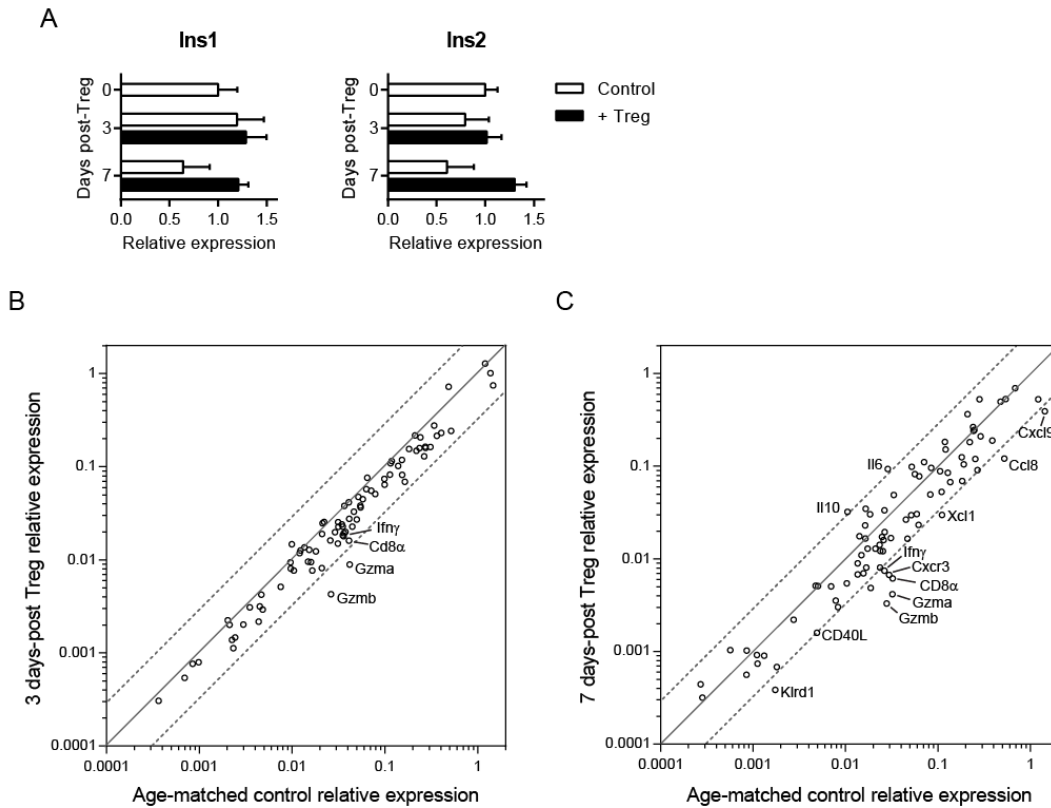
Figure 2. Tregs rapidly control diabetes progression while down-regulating a CTL signature in the islets.

mRNA was isolated for transcriptional analysis from islets pooled from 4-5 NOD.CD28^{-/-} mice at the time of Treg transfer and at 3 and 7 d after Treg treatment. (**A**) Expression of insulin 1 and 2, normalized to time of treatment baseline. Data represent the average from 2 independent experiments. Bar graphs display mean + SEM. (**B, C**) Scatter plots displaying the relative abundance of mRNA transcripts in NOD.CD28^{-/-} islets at 3 d (**B**) and 7 d (**C**) following Treg treatment, as compared to age-matched controls. Dashed lines represent a 3-fold difference between groups. Data are from 2 independent experiments.
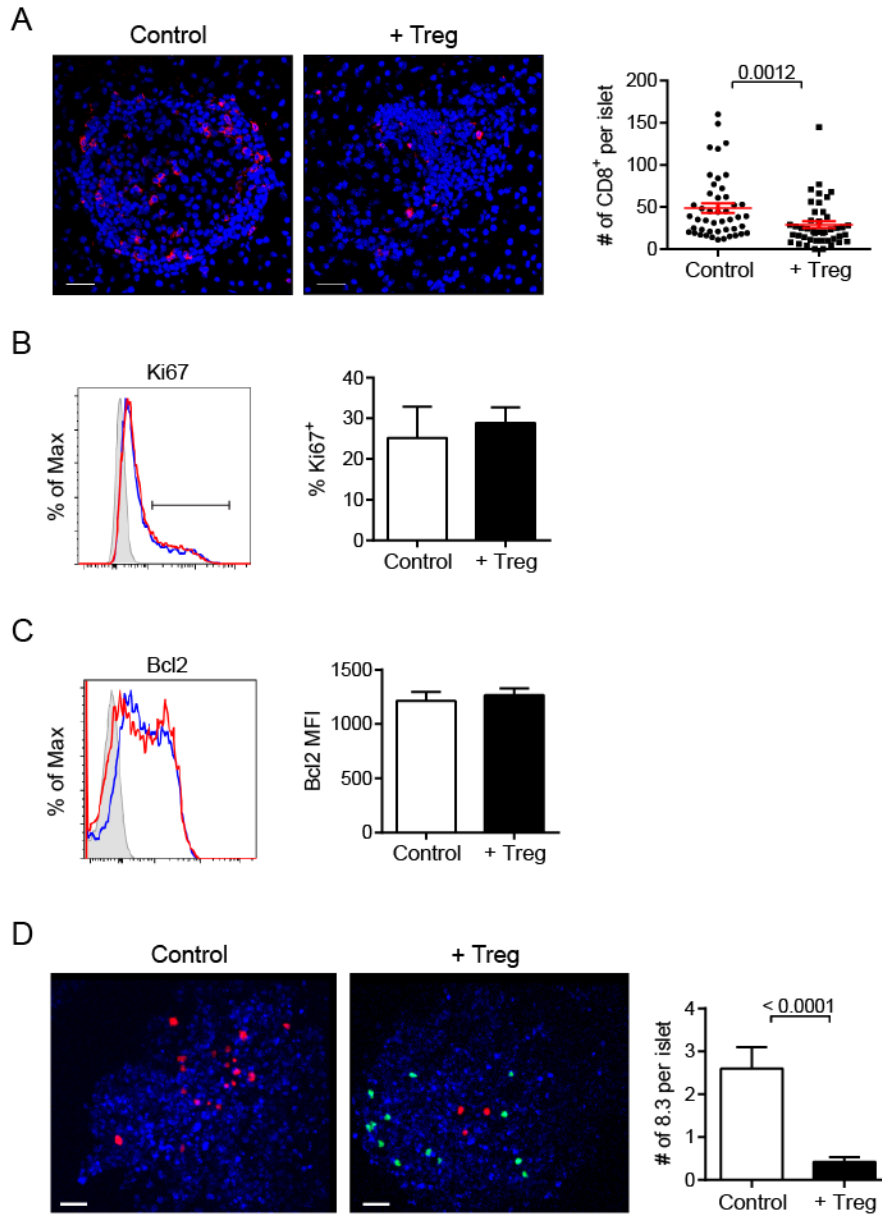
Figure 3. Tregs reduce CD8$^+$ T cell accumulation in the islets.

(**A**) Representative immunofluorescent sections showing infiltrated islets from pancreata of control and 7 d post-Treg treatment NOD.CD28$^{-/-}$ mice. CD8$^+$ T cells are shown in red and nuclei are blue. Scale bars represent 30 um. Graph depicts the number of CD8$^+$ cells counted per sectioned islet. Each dot represents one islet. Data are from over 40 islets analyzed from 3 mice for each group. Red lines represent mean + SEM. P value was

determined by Mann-Whitney test. (**B, C**) Islets were isolated from NOD.CD28$^{-/-}$ mice at 7 d post-Treg treatment and from age-matched controls for analysis by flow cytometry. Histograms overlay expression levels of Ki67 (**B**) and Bcl2 (**C**) in islet CD8$^+$ T cells of Treg-treated (red) and control (blue) mice. CD8$^+$ T cells were gated as viability dye$^-$ Thy1.2$^+$CD8$^+$. Shaded peak represents isotype control stain. Bar graphs depict the percentage of Ki67$^+$ (**B**) and the median fluorescence intensity (MFI) of Bcl2 (**C**) for islet CD8$^+$ T cells. Data represent the mean + SEM of 6 mice per group from 2 independent experiments. No statistically significant differences were observed for B or C by Student's t test. (**D**) 10^7 CMTMR-labeled CD8$^+$ T cells isolated from the spleens of NOD.8.3 TCR transgenic mice were transferred to NOD. CD28$^{-/-}$ mice at 7 d post-uGFP.BDC2.5 Treg treatment and to untreated littermate controls. Islets were harvested the following day, labeled with Hoechst, and imaged by two-photon microscopy. Representative maximal projection images show a control and Treg-treated Hoechst-labeled islet (blue) containing 8.3 CD8$^+$ T cells (red) and BDC2.5 Tregs (green, Treg-treated only). Scale bars represent 30 um. Bar graph quantifies the number of 8.3 CD8$^+$ T cells per islet. Data are from 2 independent experiments with greater than 60 total islets analyzed per group. P value was determined by Mann-Whitney test.
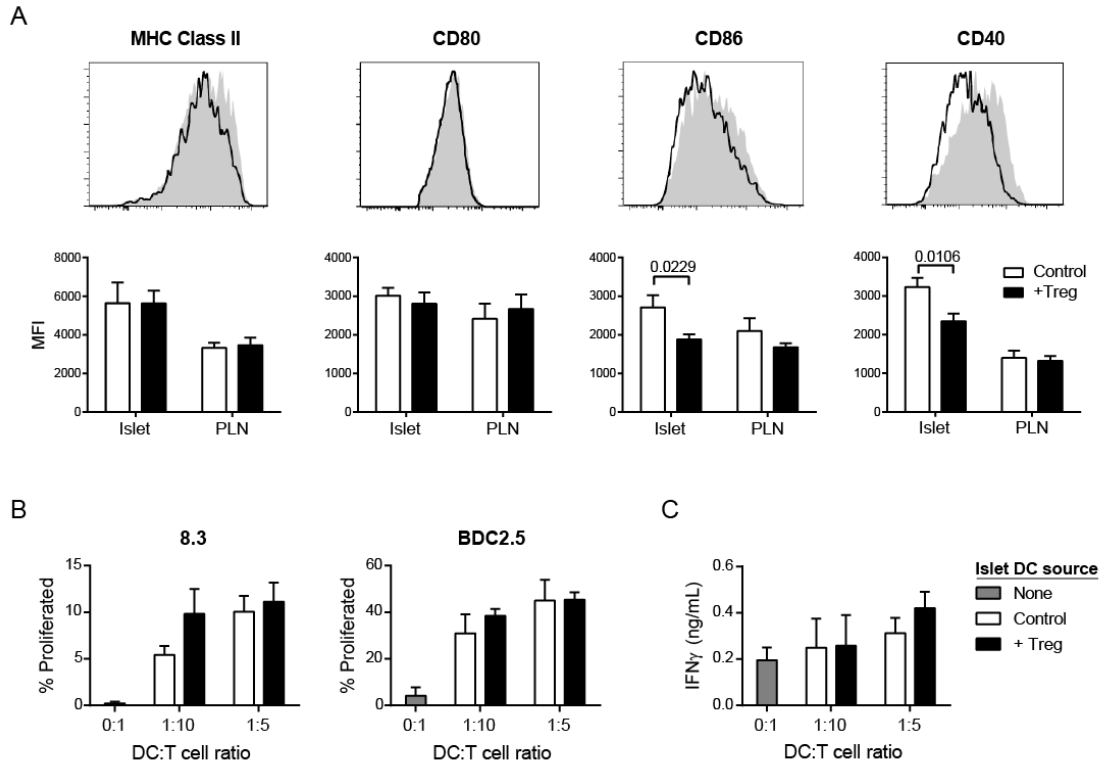
Figure 4. Phenotypic changes in islet DCs following Treg treatment do not impact their stimulatory capacity.

(**A**) Isolated islets and PLNs from NOD.CD28$^{-/-}$ mice at 7 d post-BDC2.5 Treg treatment and from age-matched controls were dissociated and analyzed by flow cytometry. Histograms depict expression levels of the indicated molecules on islet DCs in control (shaded) versus Treg-treated (outline) mice. DCs were gated as CD45^{+}CD11c^{+}B220^{-} DAPI^{-}. Bar graphs depict median fluorescent intensities. Data represent mean + SEM of 6-10 mice per group from 2-3 independent experiments. P values were determined by Student's t test. (**B, C**) NOD.CD28$^{-/-}$ mice were treated or not with 10^6 BDC2.5 Tregs. 7 d later, DCs were isolated from islets and placed in co-culture for 4 d with CFSE-labeled 8.3 and BDC2.5 T cells at a DC to T cell ratio of 1 to 10 or 1 to 5. (**B**) The percentage of 8.3 CD8^{+} T cells (left) and of BDC2.5 CD4^{+} T cells (right) that had proliferated, as

indicated by dilution of CFSE, is displayed for T cells cultured alone or with islet DCs from either control or Treg-treated islets. (**C**) Supernatants were collected at the end of the 4 d culture, and IFNγ concentrations were analyzed by ELISA. Graphs depict means + SEM for islet DCs from 4-6 individual mice per group from 2 independent experiments. No statistical differences were observed between islet DCs from control versus Treg-treated mice by ANOVA.
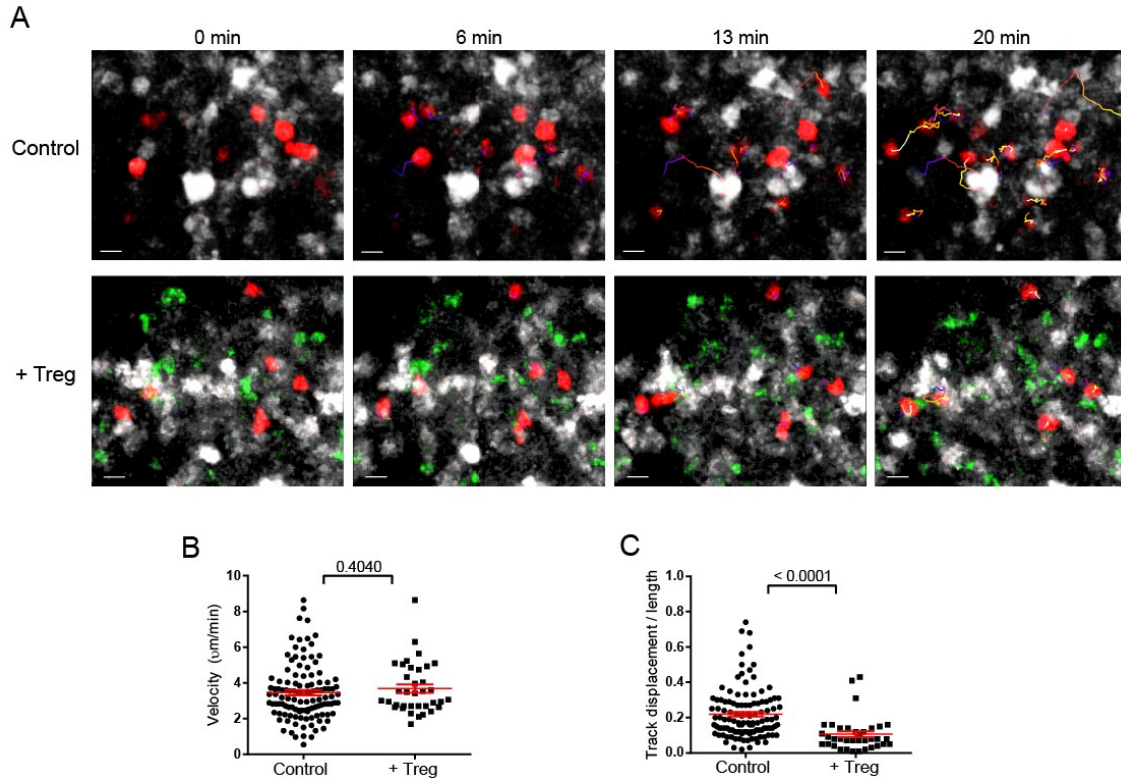
Figure 5. Tregs do not inhibit islet T cell-DC interactions.

10^7 CMTMR-labeled CD8$^+$ T cells isolated from the spleens of TCR transgenic NOD.8.3

mice were transferred to NOD.CD11c-YFP.CD28$^{-/-}$ mice at 7 d post-uGFP.BDC2.5 Treg

treatment and to untreated controls. Islets were harvested the following day and imaged

by two-photon microscopy. (**A**) Maximal projection time-lapse images from control and

Treg-treated islets depicting CD11c$^+$ DCs (white), 8.3 CD8$^+$ T cells (red), and BDC2.5

Tregs (green, + Treg only). Track lines depict 8.3 CD8$^+$ T cell movements over the

course of the 20 min imaging period and are color-coded according to time (blue at the

beginning of the imaging period to white at the end). Scale bars represent 10 um. See

Videos 2 and 3 for full time lapses. (**B, C**) Graphs depict velocities (**B**) and confinement

ratios (**C**) of 8.3 CD8$^+$ T cells. Each point represents a single cell, red bars represent

mean + SEM. Data are from multiple islets imaged over 2 independent experiments. P

values were determined by Mann-Whitney test.
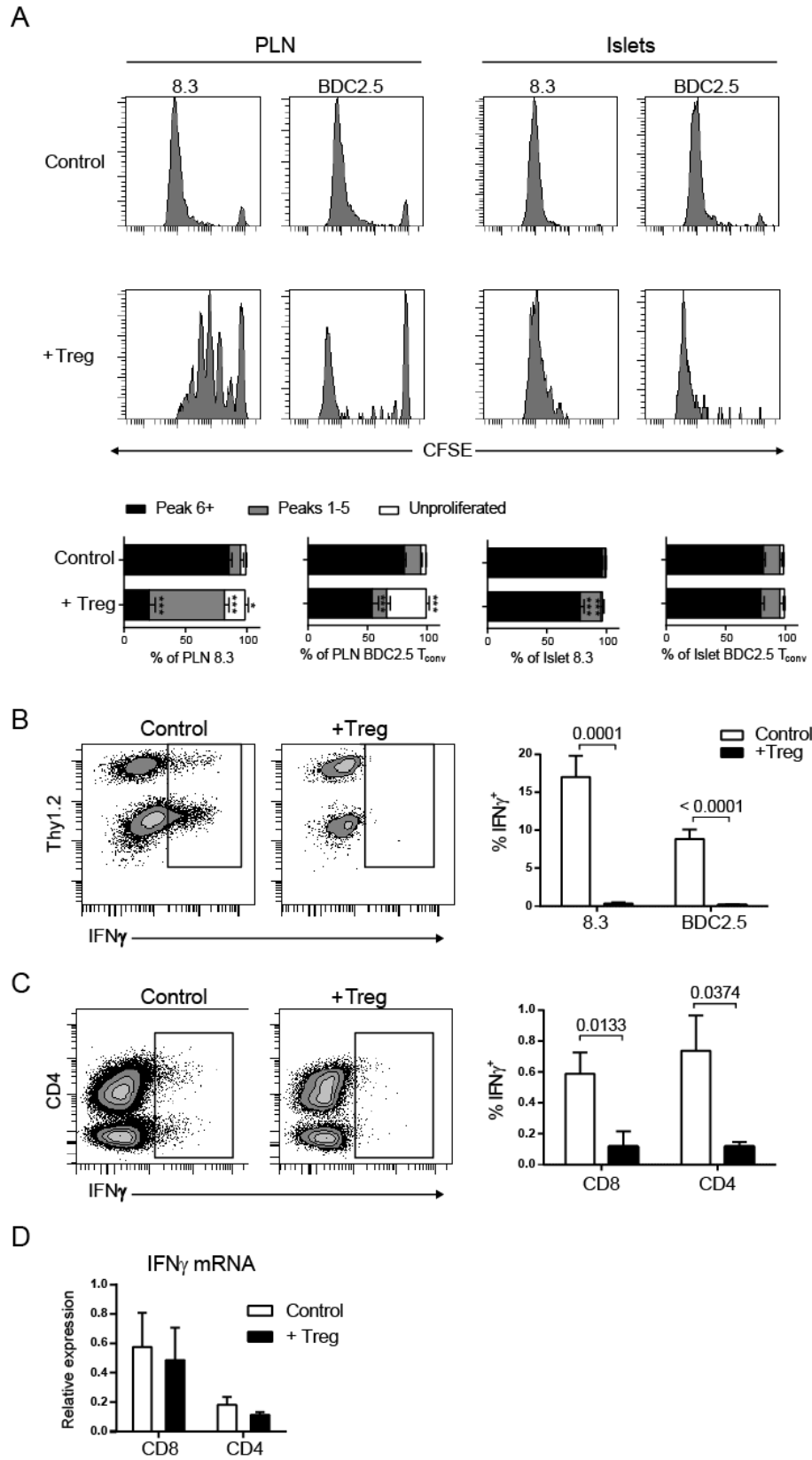
Figure 6. Tregs suppress islet T cell effector function.

(**A-C**) 10^6 CFSE-labeled 8.3.Thy1.1$^+$ CD8$^+$ T cells and 10^6 CFSE-labeled

BDC2.5.Thy1.1/1.2$^+$ CD4$^+$CD25$^-$ T cells were transferred to NOD.CD28$^{-/-}$ mice 3 d

following BDC2.5.Thy1.1$^+$ Treg treatment or to untreated littermates. 4 d later, mice

were i.v. injected with 250 ug of BFA 4 h prior to sacrifice, followed by islet isolation

and culture in the presence of BFA. (**A**) Representative histograms gated on Thy1.1$^+$

CD8$^+$ 8.3 T cells and Thy1.1/1.2$^+$CD4$^+$ BDC2.5 T cells depicting CFSE dilution of

transferred cells in the draining PLN (left) and islets (right) with and without Treg

treatment. Bar graphs depict the percentage of cells that did not divide (Unproliferated),

underwent 1-5 rounds of division (Peaks 1-5), or underwent 6 or more rounds of division

(Peak 6+). Bonferroni's multiple comparison test, *, $P < 0.05$, ***, $P < 0.0001$. (**B**)

Representative flow plots gated on Thy1.1$^+$ transferred 8.3 CD8$^+$ (Thy1.2$^-$) and BDC2.5

CD4$^+$ (Thy1.2$^+$) cells in the islets and quantification of the percentage of each cell type

that are IFNγ$^+$ by intracellular flow cytometry. (**C**) Representative flow plots gated on

endogenous islet Thy1.2$^+$Thy1.1$^-$ CD4$^+$ and CD8$^+$ T cells and quantification of the

percentage of endogenous islet T cells expressing intracellular IFNγ$^+$. Data for A-C

represent 6 mice per group from 2 independent experiments. Bar graphs depict mean +

SEM. P values for B and C were determined by Student's t test. (**D**) qRT-PCR data

measuring transcript levels of IFNγ for CD8$^+$ and CD4$^+$ T cells sorted from pooled islets

of 3-4 NOD.CD28$^{-/-}$ mice at 7 d post-Treg treatment or from age-matched controls.

Expression levels are normalized to 18s rRNA expression. Data are represented as the

mean + SEM of 4 independent experiments. No statistically significant difference was

observed between control and Treg-treated samples by paired Student's t test.
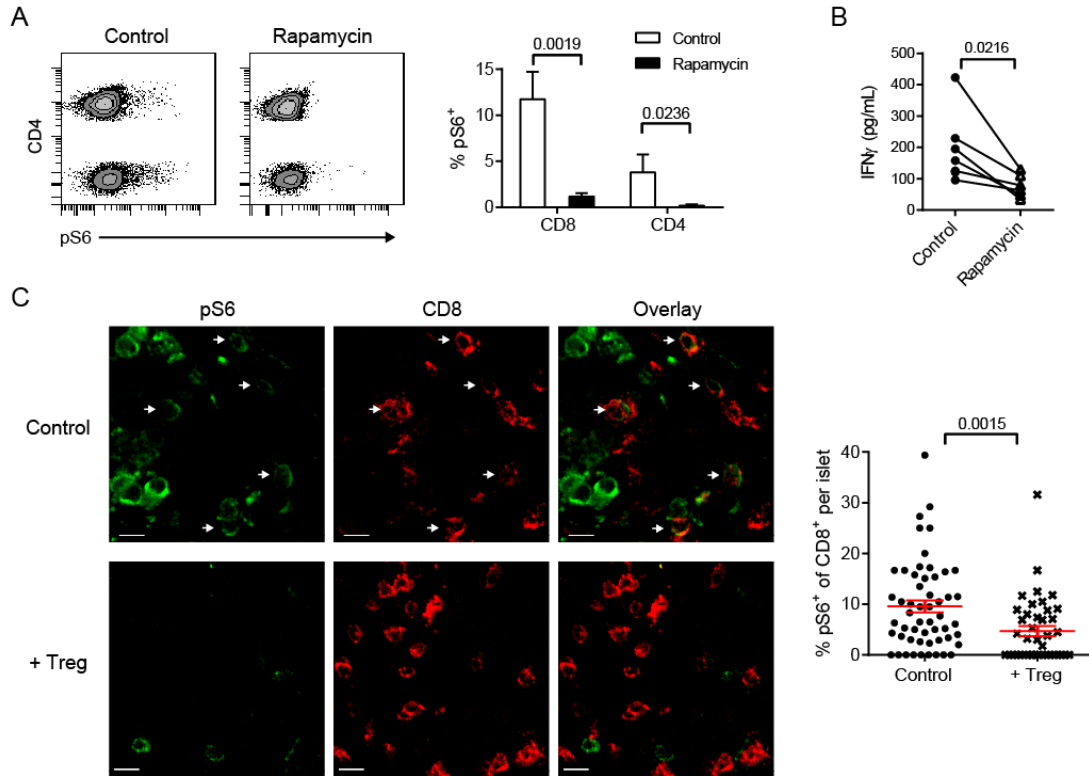
Figure 7. Tregs suppress mTOR signaling in islet CD8$^+$ T cells that is critical for IFNγ production.

(**A**) Representative flow plots gated on Thy1.2$^+$CD4$^+$ and CD8$^+$ T cells from isolated islets of NOD.CD28$^{-/-}$ mice that were dissociated and cultured overnight in the presence or absence of 100 ng/ml rapamycin. Graph depicts the mean percentages of T cells expressing pS6 + SEM. (**B**) Concentrations of IFNγ in culture supernatants as determined by ELISA. Each connected pair of data points represents cells from one mouse split into the two conditions. Data for A and B are from 6 mice from 3 independent experiments. P values were determined by paired Student's t tests. (**C**) Representative immunofluorescence images of stained pancreas sections from NOD.CD28$^{-/-}$ mice at 7 d post-BDC2.5 Treg treatment or from untreated littermates. pS6 signal is indicated in green and CD8$^+$ T cells are shown in red. White arrows highlight

51

co-expression. Scale bars represent 10 um. Graph quantifies the percentage of CD8$^+$ T cells per islet examined expressing pS6. Data are combined from 3 independent experiments with a total of 3 mice for each condition. Each point represents an individual islet with lines at means + SEM. P value was determined by Mann-Whitney test.

CHAPTER III: RECRUITMENT OF DENDRITIC CELLS TO INFLAMED ISLETS AND THE EFFECTS OF THERAPEUTIC TREGS

Abstract

Dendritic cells (DCs) play an important role in the progression of autoimmune diabetes in the NOD mouse. In this study we examined the dynamics of pancreatic islet DCs during homeostasis, destructive inflammation, and Treg-controlled inflammation. We observed heightened numbers of islet DCs upon induction of tissue inflammation. No increase in local DC proliferation was observed; rather, this increase was due to enhanced recruitment of DC precursors from the periphery that coincided with increased islet expression of inflammatory chemokines. Under inflammatory conditions, islet DCs arose primarily from a circulating monocyte precursor whose recruitment was partially dependent on Ccr5. We also examined the effects of islet-antigen specific BDC2.5 Treg treatment of pre-diabetic mice on islet DC dynamics. BDC2.5 Treg treatment halts diabetes progression without completely clearing islet immune infiltrate. Treg treatment led to an eventual reduction in islet DC numbers that was a result of decreased precursor recruitment, corresponding with reduced expression of inflammatory chemokines by infiltrated islets. Together, our results provide new insights into the source and entry of DCs at the site of an ongoing autoimmune response and how the influx of these disease-driving cells is interrupted by therapeutic Tregs.

Introduction

Dendritic cells (DCs) are critical mediators of both innate and adaptive immunity. Integrating signals from their environment, they can take on tolerogenic or immunogenic properties, thus shaping the responses of T cells recognizing peptide-MHC complexes on their surface. Given their capacity to initiate and shape immune responses, it is unsurprising that DCs play an integral role in the pathogenesis of many autoimmune diseases, including type 1 diabetes (T1D) (Ganguly et al., 2013). Much of our understanding of the role of DCs in T1D comes from studies of the non-obese diabetic (NOD) mouse, a widely-used model that spontaneously develops autoreactive immune infiltrates in pancreatic islets, resulting in diabetes (Anderson and Bluestone, 2005b). DCs are the only immune cells present in healthy islets and are among the first cells recruited at the initiation of disease (Calderon et al., 2008; Jansen et al., 1994; Shinomiya et al., 2000). Islet DCs constitutively present beta cell antigens, even in the absence of islet inflammation (Calderon et al., 2008). DCs are heavily recruited to inflamed islets over the course of disease progression (Melli et al., 2009), and depletion of DCs clears islet infiltrates and delays diabetes development (Nikolic et al., 2005; Saxena et al., 2007). Together, these findings indicate an essential role for DCs in T1D pathogenesis and suggest that disrupting islet DC influx could be a means of controlling disease. The factors driving DC recruitment to the site of inflammation remain unknown however and are likely influenced by the identity of the islet DC precursor cell.

DCs arise from diverse origins that vary depending on the particular subset, location, and inflammatory status under consideration (Geissmann et al., 2010; Satpathy et al., 2012). Under steady-state conditions, classical lymphoid tissue DCs (cDCs) arise from a bone marrow-derived hematopoietic precursor cell called the pre-cDC (Liu et al.,

54

2009). In most nonlymphoid tissues, DCs fall into two distinct subsets: CD103$^+$ cDC and

CD11b$^+$ cDC (Ginhoux et al., 2009). CD103$^+$ DCs appear to arise primarily from pre-DC

precursors (Ginhoux et al., 2009; Yin et al., 2012); although blood monocytes are also

able to contribute to this population (Geissmann et al., 2003; Jakubzick et al., 2008b).

CD103$^+$ nonlymphoid-tissue DCs share a gene signature with CD8$^+$ lymphoid-tissue DCs

(Miller et al., 2012) and the two cell types share a common dependence on the

transcription factor BATF3 (Edelson et al., 2010), indicating that they are derived from a

distinct lineage subset. In contrast, CD11b$^+$ nonlymphoid tissue DCs appear to be more

heterogeneous than their CD103+ counterparts, arising from both pre-DCs and

monocytes (Geissmann et al., 2003; Ginhoux et al., 2009; Jakubzick et al., 2008b; Yin et

al., 2012). This heterogeneity is also reflected at the transcriptional level. Microarray

profiling as part of the ImmGen project has shown that nonlymphoid tissue CD11b$^+$ DCs

distribute across the spectrum between cDCs and macrophages (Miller et al., 2012). In

the pancreatic islets, the majority of DCs under both steady-state and inflammatory

conditions are CD11b$^+$ (Calderon et al., 2008; Ginhoux et al., 2009; Yin et al., 2012).

Experiments using lineage-tracing mice have suggested that this subset arises from a

monocytic precursor in the steady-state (Yin et al., 2012).

     In inflamed tissues, DC origins are less clear. While some inflammatory DCs still

arise from pre-DC precursors, circulating blood monocytes have also been shown to give

rise to DCs in inflammatory settings, particularly those of the CD11b$^+$ subset. Monocyte

recruitment to sites of inflammation has been shown to be mediated by their expression

of chemokine receptors for inflammatory CC-family chemokines, particularly Ccr1,

Ccr2, and Ccr5 (Shi and Pamer, 2011). The specific chemotactic factors driving the recruitment of DC precursors to the islets during inflammation remain unknown.

Under steady-state conditions, regulatory T cells (Tregs) play a role in regulating DC numbers, as the two populations maintain a balance. Treg depletion in Foxp3-DTR mice results in an increase in DC numbers in secondary lymphoid organs in a Flt3-L-dependent manner (Liu et al., 2009). Conversely, expansion of DCs via Flt3L treatment also expands Tregs (Darrasse-Jeze et al., 2009). In contrast however, constitutive DC ablation results in only a moderate reduction in Treg numbers without obvious functional effects on T cell homeostasis (Birnberg et al., 2008). Unknown is whether a similar balance exists between Treg and nonlymphoid-tissue DC numbers during an inflammatory condition such as chronic autoimmunity. In the pancreatic islets of pre-diabetic NOD mice, Treg numbers and function decline with disease progression (Tang et al., 2008), while DC numbers increase (Melli et al.). Whether therapeutic Tregs might target DC numbers remains to be determined.

In this study, we investigated the precursor and origin of inflamed islet DCs and sought to identify the chemotactic factors responsible for their recruitment to the inflamed tissue. Our data show that DCs in inflamed islets arise from a Ly6c^{lo} monocyte precursor that is recruited to the tissue in a Ccr5-dependent fashion. We also investigated the impact of therapeutic Treg treatment on islet DCs in pre-diabetic mice. We found that Tregs contributed to a decrease in islet DC numbers by direct and indirect means: by killing islet DCs and by altering the chemotactic milieu to decrease islet DC recruitment. Together, these results elucidate the mechanisms of DC recruitment to inflamed islets and how this process is inhibited by therapeutic Tregs.

Materials and Methods

Mice

NOD.Rag2$^{-/-}$, NOD.CD28$^{-/-}$, NOD.CD11c-YFP.CD28$^{-/-}$, NOD.BDC2.5.Thy1.1 TCR

transgenic, and NOD.uGFP.BDC2.5 TCR transgenic mice were housed and bred under

specific pathogen-free conditions at the University of California Animal Barrier Facility.

The Institutional Animal Care and Use Committee of University of California approved

all experiments.

Islet isolation

Pancreas was perfused with 3 ml of HBSS (Hyclone) containing 0.8 mg/ml collagenase P

(Roche) via cannulated common bile duct (Lenschow et al., 1995). The distended

pancreas was excised, incubated at 37°C for 16 min, and gently tapped to release islets.

Pancreatic islets were further purified by Histopaque-1119 (Sigma-Aldrich) density-

gradient centrifugation and handpicked under a dissecting microscope.

BrdU labeling

Mice were i.p. injected with 2.5 mg BrdU 4 h prior to sacrifice. Samples were stained for

flow cytometric analysis using a FITC BrdU flow kit according to the manufacturer's

protocol (BDBiosciences).

qRT-PCR array

Handpicked islets were lysed in TRIzol (Invitrogen). mRNA was extracted using RNeasy Micro columns (QIAGEN). Reverse transcription was done using SuperScript III (Invitrogen). qRT-PCR used SYBR Green Mastermix (SABiosciences) on the Bio-Rad CFX 96 platform. An RT^2 Profiler Custom PCR Array (SABiosciences) was used to simultaneously examine transcript levels of 86 genes selected for their relevance to T1D, along with 4 housekeeping genes and controls for genomic DNA contamination, RNA quality and general PCR performance.

Chemokine protein concentration

Isolated islets were cultured overnight at 37° in 5% CO_2 in a non-tissue culture-treated plate in RPMI + 10% FCS at a density of 2 ul of media per islet. Islets and supernatants were collected the following day and snap frozen in liquid nitrogen. Samples were then thawed, sonnicated 10x 30 sec to homogenize, and centrifuged 10 min at 14,000 rcf. Supernatants of this lysate were used for protein analysis.

Bead-tracking of blood monocytes

1 um green fluorescent microspheres (Polysciences Inc) were diluted 1 to 4 in PBS. 250 ul of the diluted bead solution were retro-orbitally injected to recipient mice. When labeling Ly6c^{hi} blood monocytes, recipient mice were i.v. injected with 250 ul of clodronate liposomes (ClodronateLiposomes.com) the day before bead injection.

5-FU chimeras

5-FU (Sigma) was freshly prepared at 10 mg/ml in PBS on the day of injection. Mice were i.p. injected with 150 mg/kg 5-FU. Bone marrow cells were harvested from donor mice the following day. Briefly, femurs and tibias were flushed of bone marrow that was sheared into a single cell suspension using a syringe. Following red blood cell lysis with ACK lysing buffer (Lonza), cells were washed, resuspended in PBS, and i.v. injected to 5-FU pre-treated recipients at a dose of 2-3 x 10^7 bone marrow cells per mouse. Animals were sacrificed d 14 post-bone marrow transfer at which time blood and islets were harvested for flow cytometric analysis.

Flow cytometry

Handpicked islets were dissociated into single cells by incubating in Gibco Cell Dissociation Buffer (Invitrogen) for 30 min in a 37°C water bath, followed by mechanical disruption by pipetting up and down. Cells were then filtered and washed before staining. Blood samples were collected into 20 U/ml heparin and leukocytes were isolated by Ficoll gradient centrifugation. Analyses were performed on a LSRII or Fortessa flow cytometer (BD Biosciences) with FACSDiva analysis software (BD Biosciences).

Two-photon imaging

Handpicked islets were stained in 5 ug/ml Hoechst for 15 min at room temperature and embedded in RPMI medium containing 0.5% low melting point agarose (Invitrogen) on a plastic coverslip. The embedded islets were placed in a flow chamber perfused with RPMI medium without phenol red saturated with 95% O_2/5% CO_2. Temperature within

the chamber was maintained between 36 and 37°C during the entire imaging period.

Images were acquired on a custom-built 4 PMT detector video-rate two-photon

microscope using a water immersion 20x/0.95 NA objective with the aid of

Micromanager software. For time-lapse image acquisition, *z*-stacks with up to 40 *xy*

planes with 5 um spacing were acquired every 30 or 60 s for 20-60 min. Data were

visualized and analyzed using Imaris software (Bitplane AG).

Cell transfers

For BDC2.5 Treg treatments, FACS-purified CD4$^+$CD62L^{high}CD25$^+$ Tregs from lymph

nodes of NOD.BDC2.5.Thy1.1 TCR transgenic mice were expanded with anti-

CD3/CD28 coupled Dynabeads (Invitrogen) for 10 days in the presence of 2000 IU/ml

rhIL-2 in DMEM and 10% FCS as previously described (Tang et al., 2004). Purity of the

culture was determined at the end of the expansion by analyzing an aliquot for Foxp3

expression using flow cytometry. BDC2.5 Treg-treated mice were i.p. injected with 10^6

of the *ex vivo* expanded BDC2.5 Tregs at 5 to 7 weeks of age. For two-photon imaging

experiments at 18 h – 3 days post-Treg transfer, 3-5 x 10^6 BDC2.5 Tregs were labeled

with CMTMR (Invitrogen) and i.v. injected. For two-photon imaging experiments at day

7 post-Treg transfer, NOD.uGFP.BDC2.5 mice were used as the source of Tregs, with

isolation and expansion as above, followed by injection of 10^6 Tregs.

For BDC2.5 Teff transfers, FACS-purified CD4$^+$CD62L^{high}CD25$^-$ T cells from

lymph nodes of NOD.BDC2.5.Thy1.1 TCR transgenic mice were expanded with anti-

CD3/CD28 coupled Dynabeads (Invitrogen) for 10 days in the presence of 2000 IU/ml

rhIL-2 in DMEM and 10% FCS. 10^6 of the *ex vivo* expanded BDC2.5 Teffs were i.p. injected per mouse.

Statistical analysis

Statistical analyses were performed with the aid of Prism software (GraphPad) using the tests indicated.

Results

CC-family chemokines are highly induced in inflamed islets

Our previous studies have shown a rapid increase in islet DC numbers in an adoptive transfer model of intra-islet inflammation where BDC2.5 CD4^{+}CD25^{-} effector T cells (Teffs) are transferred to NOD.Rag2^{-/-} mice to induce islet inflammation. This increase in islet DCs is not due to DC proliferation as measured by Ki67 staining (Melli et al., 2009). We further corroborated that the increase in islet DC numbers upon induction of inflammation is not due to proliferation by short-term BrdU labeling experiments that showed no increased uptake of BrdU in DCs from inflamed islets versus non-inflamed islets (**Fig. 1 A**). In fact, islet DCs in mice that received BDC2.5 Teffs had significantly lower levels of BrdU incorporation than non-inflamed untreated controls. In parallel to our adoptive transfer model, we have also examined islet DCs in a model of spontaneous islet infiltration. NOD.CD28^{-/-} mice develop rapid and aggressive diabetes as a result of their extreme deficit in functional Tregs (Salomon et al., 2000). Islets of these mice contain large numbers of DCs during the pre-diabetic stages. Similar to our

observations in the adoptive transfer model, islet DCs in the inflamed islets of NOD.CD28$^{-/-}$ mice showed low levels of BrdU incorporation, indicating that *in situ* DC proliferation likely does not contribute to the maintenance of high numbers of DCs in this model of spontaneous and rapid islet inflammation (**Fig. 1 A**).

Having ruled out local proliferation as a primary contributor to the increase in islet DCs during inflammation, we next focused on the recruitment of these cells to the tissue. Recruitment of DCs into inflamed islets is likely orchestrated by increased expression of chemokines and adhesion molecules. To test this hypothesis, we surveyed the expression of a large panel of chemokines and adhesion molecules at the transcriptional level using a custom-designed 96-well qPCR array. mRNA was extracted from isolated islets of pre-diabetic NOD.CD28$^{-/-}$ mice at various time points during disease progression and from islets of non-inflamed NOD.Rag2$^{-/-}$ mice. A number of inflammatory CC-family chemokines that are involved in recruiting myeloid cells to sites of inflammation were highly induced in inflamed NOD.CD28$^{-/-}$ islets as compared to NOD.Rag2$^{-/-}$ controls. These included Ccl2, Ccl5, Ccl7, Ccl8, and Ccl9, all of which were upregulated greater than 5-fold in NOD.CD28$^{-/-}$ islets for at least one of the multiple time points examined (**Fig. 2 A**). Ccl2, although highly upregulated at 5 weeks of age, did not persist in being highly expressed at later ages as disease progressed. In contrast, Ccl5 consistently showed high levels of upregulation in NOD.CD28$^{-/-}$ islets at all ages examined. In contrast to the upregulation of inflammatory chemokines in inflamed versus non-inflamed islets, expression levels of adhesion molecules were mainly unaltered (data not shown). Chemokines were further examined at the protein level. Isolated islets were cultured overnight, collected with culture supernatant and

homogenized, and analyzed in luminex and ELISA assays. In agreement with our mRNA data, Ccl2, Ccl5, and Ccl8 were observed at high levels in supernatants from cultured NOD.CD28$^{-/-}$ islets as compared to NOD.Rag2$^{-/-}$ islets, while Ccl3 and Ccl4 were expressed at low levels regardless of islet inflammation (**Fig. 2 B**). These data provided candidate chemokines putatively involved in DC recruitment to inflamed islets for further investigation.

Islet DCs arise from Ly6c^{lo} blood monocytes

We next sought to identify the precursor of inflamed islet DCs. In NOD mice, the majority of DCs in infiltrated islets are CD11b^{+}, with only a minor subset being CD103^{+}CD11b^{-}. As such, we chose to focus specifically on CD11b^{+} islet DCs. Previous work by others has found steady-state islet CD11b^{+} DCs to be GFP^{+} in *LysM-Cre x Rosa26-floxstop-floxEGFP* mice, where GFP is expressed in cells that have at one time expressed the monocyte marker LysM, suggesting that these cells are derived from a monocyte precursor (Yin et al., 2012). In mice, blood monocytes can be divided into two subpopulations based on their expression levels of Ly6c, both of which are labeled in the LysM-cre mouse (Jakubzick et al., 2008a). In the setting of islet inflammation, whether CD11b^{+} DCs are still monocyte derived and the particular monocyte subset that gives rise to CD11b^{+} DCs has not been identified. To address this, we employed a method previously developed by the Randolph group to label specific blood monocyte populations and track their possible appearance in the islets of pre-diabetic NOD.CD28$^{-/-}$ mice. Fluorescently labeled latex beads injected directly into the bloodstream are rapidly taken up by Ly6c^{lo} blood monocytes that can be detected for 5-7 days in the circulation

((Tacke et al., 2006) and **Fig. 3 A and C**). Flow cytometric analysis of inflamed islets at 3 to 5 days post-bead injection revealed that the majority of bead-labeled cells in the islets were in the CD11c$^+$CD11b$^+$ DC population (**Fig. 3 B and D**). These data suggest that Ly6c^{lo} blood monocytes are recruited to inflamed islets where they can differentiate into islet DCs.

Our finding that Ly6c^{lo} monocytes give rise to DCs in an inflamed tissue is somewhat surprising, as Ly6c^{hi} monocytes are typically considered to be the inflammatory monocyte subset and to be more likely to give rise to inflammatory DCs (Geissmann et al., 2003; Rivollier et al., 2012; Varol et al., 2009). The finding that Ly6c^{lo} monocytes can also differentiate into inflamed DCs is not without precedent however, as Tacke et al. have reported similar findings in a mouse model of atherosclerosis (2007). To also measure the ability of Ly6c^{hi} blood monocytes to give rise to DCs in inflamed islets, we employed a variation of the bead labeling method that leads to labeling of Ly6c^{hi} instead of Ly6c^{lo} monocytes. By initially depleting monocytes with i.v. injection of clodronate liposomes, beads are taken up preferentially by the Ly6c^{hi} subset upon their recovery (Tacke et al., 2006). Using this approach, bead-labeled monocytes in the blood at day 5 post-injection were primarily Ly6c^{hi}, although some had begun to convert to the Ly6c^{lo} subset by this time-point (**Fig. 3 C**). In the islets of these mice, bead-labeled cells were predominately CD11b$^+$CD11c$^-$ myeloid cells, while a smaller subset was contained within the CD11c$^+$CD11b$^+$ DC population (**Fig. 3 D**). Given the conversion of some bead-labeled monocytes to the Ly6c^{lo} subset at this timepoint however, it is probable that these bead-labeled islet DCs arose from the Ly6c^{lo} population rather than directly from a Ly6c^{hi} precursor. In order to more definitively

determine whether Ly6c^{hi} monocytes can give rise directly to islet DCs, ongoing experiments will examine islets at 3 days following bead injection using the Ly6c^{hi} labeling method, when bead-labeled cells will have had less time to convert to the Ly6c^{lo} subset. Based on the above observations, we conclude that Ly6c^{lo} blood monocytes are precursors of inflamed islet DCs.

Islet DC recruitment is dependent on Ccr5

We next sought to pinpoint the specific chemokine receptor(s) involved in the trafficking of DC precursors to inflamed islets. Ly6c^{lo} blood monocytes express Cx3cr1 and have been shown to use Ccr5 to enter inflamed atherosclerotic plaques where they differentiate into CD11c$^+$ cells (Tacke et al., 2007). Islet DCs have been reported to express Ccr5 (Calderon et al., 2008) and Ccr5 was upregulated at the message level in NOD.CD28$^{-/-}$ whole islet mRNA as compared to non-inflamed NOD.Rag2$^{-/-}$ islets (data not shown). Additionally, the Ccr5 ligand, Ccl5, was highly upregulated in inflamed islets (**Fig. 2 A and B**). These data led us to form the hypothesis that islet DC recruitment is Ccr5-dependent under inflammatory conditions. To test this, we developed a novel assay that creates short-term, partial bone marrow chimeras by treating mice with the chemo-ablative agent 5-fluorouracil (5-FU) followed by injection of Ly5.2 congenically marked bone marrow cells (outlined in **Fig. 4 A**). Treatment with 5-FU enabled the engraftment of the transferred donor cells without disrupting pre-existing islet infiltrate. Unlike radiation-generated chimeras, this method did not disrupt diabetes progression, as demonstrated by similar diabetes incidence in 5-FU chimeric and untreated control NOD.CD28$^{-/-}$ mice (**Fig. 4 B**). When examining the accumulation of

donor bone marrow-derived leukocytes in the periphery, we saw that myeloid cells reached high levels of peripheral chimerism at two weeks post-bone marrow transfer.

Donor derived monocytes and other myeloid cells appeared in the periphery of recipient animals by day 7-post bone marrow transfer and peaked around 2 weeks post-transfer. Since host islet DCs were not deleted by the 5-FU treatment and host monocytes persist in the periphery, percentages of Ly5.2$^+$ donor DCs in the islets reflect the accumulation of a portion of the newly recruited DCs during the one week period between the time donor cells appear in the circulation on day 7 and the time of analysis on day 14. In non-inflamed NOD.Rag2$^{-/-}$ mice, the percentages of donor DCs in islets increased with higher percentages of donor myeloid cells in the blood (**Fig. 4 C**), showing that the overall level of chimerism in the circulation affects the percentage of donor DCs in islets. Overall, the percentages of donor DCs present in NOD.Rag2$^{-/-}$ islets at the end of the two-week assay were between 5 to 29%. This low level of donor DCs is likely due to the low rate of islet DC turnover and recruitment of new DCs under steady-state conditions. However, in NOD.Rag2$^{-/-}$ mice in which islet inflammation was induced by transfer of activated BDC2.5 Teffs at day 7 post-bone marrow transfer, the percentage of islet DCs that were donor derived was significantly increased, despite similar levels of blood DC chimerism between BDC2.5 Teff-treated and untreated mice (**Fig. 4 C**). These results reinforced the finding that islet DCs arise from a peripheral blood precursor, the recruitment of which is increased with islet inflammation.

To test the requirement of specific chemokine receptors for DC recruitment to inflamed islets, we adapted the approach described above to make short-term mixed bone marrow chimeras following 5-FU conditioning. Recipient mice received a 50/50 mixture

of wild-type and chemokine receptor knockout bone marrow (**Fig. 4 D**). Knockout bone

marrow donors tested included Ccr2$^{-/-}$, Ccr5$^{-/-}$, and Ccr7$^{-/-}$ mice. As these knockouts were

available to us on the B6 but not the NOD background, transfers were done into

NOD.Rag2$^{-/-}$ mice to avoid rejection of the allo-mismatched cells. Bone marrow cells

were depleted of T cells prior to transfer to mitigate a GVHD response during the two-

week reconstitution period. As above, BDC2.5 Teffs were transferred at day 7 post-bone

marrow transfer to induce islet inflammation, and chimerism levels in the blood and islets

were analyzed the following week. Ccr2 is also a differentiating marker for the Ly6c^{lo}

and Ly6c^{hi} monocyte subsets, as it is preferentially expressed by the Ly6c^{hi} subset, while

Ly6c^{lo} monocytes are Ccr2^{-} and instead express Cx3cr1 (Shi and Pamer, 2011). Even

though Ly6c^{lo} monocytes do not express high levels of Ccr2, their generation from Ly6c^{hi}

monocytes makes these cells also dependent on Ccr2, which is involved in monocyte

egress from the bone marrow (Tsou et al., 2007). As a result, Ccr2$^{-/-}$ cells made up

significantly less than half of the donor bone marrow-derived blood monocytes, both

Ly6c^{lo} and Ly6c^{hi}. Due to this decreased frequency of Ccr2$^{-/-}$ monocytes in the blood, a

lower proportion of islet DCs arose from Ccr2$^{-/-}$ cells than from wild-type cells. To take

into account the decreased availability of knockout precursor cells in the blood, the ratio

of knockout to wild-type islet DCs was divided by the ratio of knockout to wild-type

Ly6c^{lo} blood monocytes. When normalized in this manner, Ccr2$^{-/-}$ cells had no

deficiency compared to wild-type cells in giving rise to islet DCs (**Fig. 4 E**). This further

supported our conclusion from the bead tracking experiments that islet DCs do not arise

from Ly6c^{hi} monocytes. In contrast, in mice that received a mixture of wild-type and

Ccr5$^{-/-}$ bone marrow, wild-type cells preferentially gave rise to islet DCs, despite

knockout cells making up a higher proportion of Ly6c^{lo} blood monocytes. The higher

proportions of knockout cells among Ly6c^{lo} monocytes but not among other blood

leukocyte populations indicated that there was a buildup of Ccr5$^{-/-}$ Ly6c^{lo} monocytes in

the bloodstream. When normalized to chimerism proportions in the blood, Ccr5$^{-/-}$ cells

gave rise to a disproportionately low numbers of islet DCs, indicating that islet DC

recruitment is dependent on Ccr5 (**Fig. 4 E**). Lastly, Ccr7$^{-/-}$ bone marrow was used as a

negative control. Ccr7 is involved in trafficking from peripheral tissues to lymph nodes

(Bromley et al.; Debes et al.), and as such we predicted that Ccr7 deficiency would not

impede cells from entering inflamed islets. In agreement with this hypothesis, mice that

received a 50/50 mix of wild-type and Ccr7$^{-/-}$ bone marrow had roughly equivalent levels

of wild-type and knockout donor-derived cells among various blood leukocyte

populations, including Ly6c^{lo} monocytes, and also among islet DCs, demonstrating the

Ccr7 is not involved in islet DC recruitment (**Fig. 4 E**). Altogether, these data indicated

that Ccr2 and Ccr7 are not involved in the recruitment of islet DCs under inflammatory

conditions, but this recruitment is partially dependent on Ccr5.

BDC2.5 Treg treatment decreases endogenous islet DC numbers

Adoptive transfer of *in vitro* expanded BDC2.5 Tregs is highly effective at

protecting against diabetes development, both in wild-type and CD28-deficient NOD

mice (Tang et al., 2004; Tarbell et al., 2007; Tarbell et al., 2004b). Since the increase in

islet DCs serves to amplify the anti-islet immune response, we asked whether Tregs

might disrupt this amplification by halting islet DC accumulation. To address this

question, we enumerated the numbers of endogenous islet DCs in NOD.CD11c-YFP

CD28$^{-/-}$ mice by two-photon imaging following BDC2.5 Treg transfer. At two weeks post-Treg transfer, islet DC numbers were reduced by approximately 65 percent as compared to untreated age-matched controls (**Fig. 5 A and B**), indicating that BDC2.5 Treg treatment leads to a reduction in islet DC numbers.

Although DCs in inflamed islets already exhibit very low levels of *in situ* proliferation (**Fig. 1**), we performed short-term BrdU labeling experiments on control and Treg-treated NOD.CD28$^{-/-}$ mice to test whether the decrease in DC numbers following Treg treatment might be due to decreases in local proliferation of islet DCs. However, the low level of DC proliferation was unaffected by Treg treatment (**Fig. 5 C**), suggesting that the decrease in DC numbers after Treg treatment is likely not due to inhibition of *in situ* DC expansion in the islets.

Another possible explanation for the decrease in islet DC numbers following Treg treatment is reduced DC survival in the presence of Tregs. Others have reported the ability of Tregs to kill target cells, but such killing has previously been difficult to detect in vivo (Cao et al., 2007; Grossman et al., 2004; Zhao et al., 2006). To explore this possibility, islets were imaged in real-time by dynamic time-lapse two-photon imaging. Fluorescently labeled BDC2.5 Tregs were transferred to NOD.CD11c-YFP.CD28$^{-/-}$ mice at 1 to 7 days before imaging. On the day of imaging, islets were isolated, embedded in low-melt agarose, and placed in a chamber with a continuous flow of warm, oxygenated media to maintain physiologic conditions for the duration of imaging. Individual islets were imaged for periods of 20 to 30 minutes. BDC2.5 Tregs were seen to engage in dynamic interactions with CD11c-YFP$^+$ DCs. In rare instances, YFP$^+$ DCs either in direct contact with or in the vicinity of a Treg lost fluorescence and disappeared (**Fig. 5 D**

and E). While this was not a frequent occurrence, such DC disappearance was almost never observed in cumulative hours of imaging DCs in multiple islets of untreated control mice (**Fig. 5 E**). These results suggested that Treg-DC interactions in the tissue occasionally result in the death of the DC. The rate of DC disappearance in Treg-treated islets was approximately 1 DC per 30 minutes. While this would eventually lead to a reduction in DC numbers in a static situation, the impact would likely be small in the face of a continuing influx of DC precursor cells from the periphery that we have observed in inflamed islets. Therefore, we next investigated the possibility that changes in islet DC number were also due to changes in recruitment of DCs to islets from the periphery.

Downregulation of DC-attracting chemokines and a concomitant reduction in DC recruitment following BDC2.5 Treg treatment

To determine if Treg treatment affected the expression of DC-attracting chemokines in the islets, mRNA was extracted from islets isolated from NOD.CD28$^{-/-}$ mice at two weeks following BDC2.5 Treg treatment, along with age-matched untreated controls. Transcriptional profiling of this mRNA using our qPCR array approach revealed that a number of the inflammatory chemokine genes upregulated in NOD.CD28$^{-/-}$ islets as compared to NOD.Rag2$^{-/-}$ islets were in turn downregulated in islets from NOD.CD28$^{-/-}$ mice two weeks post-Treg treatment as compared to their untreated age-matched controls. These included Ccl2, Ccl5, Ccl7, Ccl8, and Ccl9 (**Fig. 6 A**). Of these, Ccl5, a ligand for the DC-attracting chemokine receptor Ccr5, showed the most dramatic downregulation. When examined at the protein level, supernatants from islets of NOD.CD28$^{-/-}$ mice at two weeks post-Treg treatment had lower concentrations of Ccl5

than supernatants from islets of age-matched controls, while Ccl2 protein, a ligand for Ccr2, did not appear to be regulated by Tregs (**Fig. 6 B**). In concordance with these findings and our observed decrease in islet DC number, we also saw decreased expression of the cognate receptors Ccr1, Ccr2, Ccr5 and Ccr8 at two weeks following Treg treatment (**Fig. 6 C**). Altogether, these findings indicated that Treg treatment leads to reduced islet expression of the chemokines required for trafficking of the DC precursor into the islets.

Having seen the above reduction in islet expression of DC-attracting chemokines following Treg treatment, we next utilized our *in vivo* recruitment assays to test whether our hypothesized reduction in recruitment could be observed *in vivo*. Using the 5-FU bone marrow chimera approach, NOD.CD28$^{-/-}$ mice were either treated or not with BDC2.5 Tregs at the time of the congenic bone marrow transfer. When mice were analyzed two weeks later, those that had received BDC2.5 Tregs had significantly lower levels of donor DCs in the islets, despite comparable levels of peripheral chimerism (**Fig. 7 A**). We also measured the effects of Treg treatment on islet DC recruitment by labeling blood monocytes with fluorescent beads and tracking their appearance as DCs in the islets. In mice that received BDC2.5 Tregs 2 weeks prior to bead injection, significantly fewer bead^{+} DCs were detected per islet (**Fig. 7 B**). Together, these findings indicated that the reduction in islet expression of DC-attracting chemokines following Treg treatment resulted in a decrease in the recruitment of islet DC precursor cells into the tissue.

Discussion

71

This work has demonstrated in a model of autoimmune diabetes that islet DCs arise from Ly6c^{lo} blood monocytes. These cells are attracted to the inflamed tissue that expresses high levels of Ccl5 via the cognate receptor Ccr5. Therapeutic Tregs reduce this recruitment by decreasing islet expression of Ccl5 and other inflammatory chemokines.

The data in this study and others suggests that the convention of distinguishing Ly6c^{hi} and ^{lo} monocytes as "inflammatory" and "resting", respectively, might be misleading. While Ly6c^{lo} monocytes have the unique function of patrolling the blood stream under steady-state conditions (Auffray et al., 2007), both cell types are recruited to sites of inflammation where they give rise to macrophages and DCs. A primary difference between the two appears to be the chemokine receptors utilized for such trafficking. Ly6c^{hi} monocytes express high levels of Ccr2, which they use to traffic to sites of inflammation. In contrast, Ly6c^{lo} monocytes express low levels of Ccr2 and instead express Cx3cr1. Data from this study and others (Jakubzick et al., 2008b; Tacke et al., 2007) suggests that Ly6c^{lo} monocytes may commonly use Ccr5 as a means of trafficking to inflamed tissues. These differences are likely indicative of different functions of these two cell types upon arrival in the inflamed tissue, and may provide means to differentially target one or the other.

Data on the role of Ccr5 in the pathogenesis of diabetes in NOD mice has been mixed. In agreement our observed role for Ccr5 in the recruitment of islet DCs and disease progression, studies treating mice with a blocking Ccr5 antibody have demonstrated reduced insulitis and delayed diabetes (Carvalho-Pinto et al., 2004).

However, when backcrossed to the NOD background, Ccr5-deficient mice have been reported to have accelerated diabetes (Solomon et al., 2010). This accelerated disease actually corresponded with early infiltration by F4/80$^+$ macrophages in the pancreatic islets. Lack of Ccr5 did not completely block entry of islet DC precursors in our mixed bone marrow chimeras, suggesting compensatory or redundant mechanisms for this process. It is possible that in the complete absence of Ccr5, sole reliance on these compensatory mechanisms could alter the course of disease. Furthermore, NOD.Ccr2$^{-/-}$ mice have been reported to exhibit delayed diabetes (Solomon et al., 2010), which is somewhat surprising given our finding that Ccr2 is not required for tissue entry of islet DC precursors. As a possible explanation, it should be noted that Ccr2 is required for monocyte egress from the bone marrow (Tsou et al., 2007). In agreement with this, we saw a disproportionately low percentage of Ccr2$^{-/-}$ monocytes in the peripheral blood of our mixed chimera mice, which resulted in proportionally lower levels of Ccr2$^{-/-}$ islet DCs. In the case of NOD.Ccr2$^{-/-}$ mice, the delay in disease is likely related to this defect in monocyte egress from the bone marrow. This would result in a lack of islet DC precursors in the peripheral blood, which would in turn slow the progression of disease.

It is important to note that the decreased expression of inflammatory chemokines and the corresponding decrease in DC recruitment is not immediate following Treg treatment; rather, these effects do not robustly appear until two weeks following Treg transfer. However, Tregs are known to work rapidly upon transfer. Tregs can restore euglycemia in about a week when give to diabetic mice (Tang et al., 2004) and transcriptional profiling of Treg-treated islets has shown increases in insulin production in as little as three days following treatment. These observations suggest that Tregs take

immediate actions in the target tissue to interrupt disease progression. Indeed, other studies from our lab have shown CD8^{+} effector T cells to be among the immediate targets of Tregs. Tregs rapidly suppress IFNγ production by both CD4^{+} and CD8^{+} T cells within days of transfer (Ch. 2). This inhibition of IFNγ production may be the upstream event that leads to downregulation of inflammatory chemokines in the islets, as Ccl5, in addition to Cxcl9 and Cxcl10, has been reported to be regulated by IFNγ (Wen et al., 2010). Similarly to Ccl5, Cxcl9 and Cxcl10 were highly upregulated in inflamed islets and subsequently downregulated following Treg treatment ((Medina et al., 2012), data not shown). While these observations suggest that the reduction in islet DC numbers following Treg treatment is likely not the primary means of initial Treg control over disease progression, this reduction may very well play an important role in Treg maintenance of long-term disease control.

Altogether, this work has served to elucidate the origins of DCs in inflamed islets, as well as the mechanisms by which islet DC precursors are recruited to the inflamed tissue. That this recruitment is targeted by therapeutic Tregs further highlights the importance of these cells in propagating the autoimmune response. Targeting tissue DCs, either by blocking their recruitment or by other means, may be a useful approach in the treatment of T1D and other tissue-specific autoimmune diseases.
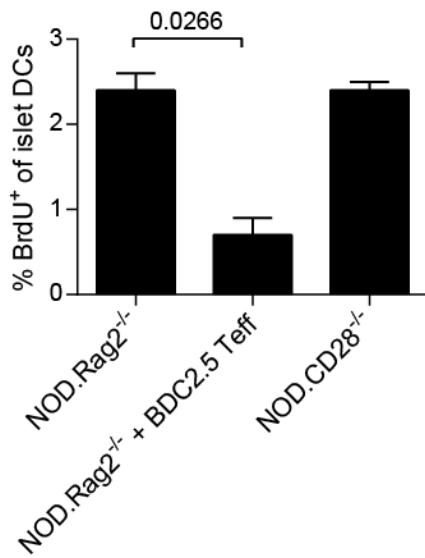
Acknowledgements

We thank V. Dang and N. Lescano for mouse husbandry; the UCSF BIDC for help with two-photon imaging; and Drs. J. A. Bluestone and J. G. Cyster for helpful discussions and critical reading of this manuscript.

<u>Footnotes</u>

Figures

Figure 1. Islet inflammation does not increase local DC proliferation.

Proliferation of islet DCs was measured by BrdU incorporation. Following a 4 h BrdU

pulse, islets were isolated for flow cytometric analysis. Islet DCs were gated as

$CD45^+CD11c^+B220^-$. Bar graph depicts mean + SEM of 2-3 mice per group from one

experiment. P value was determined by Student's t test.

A

B
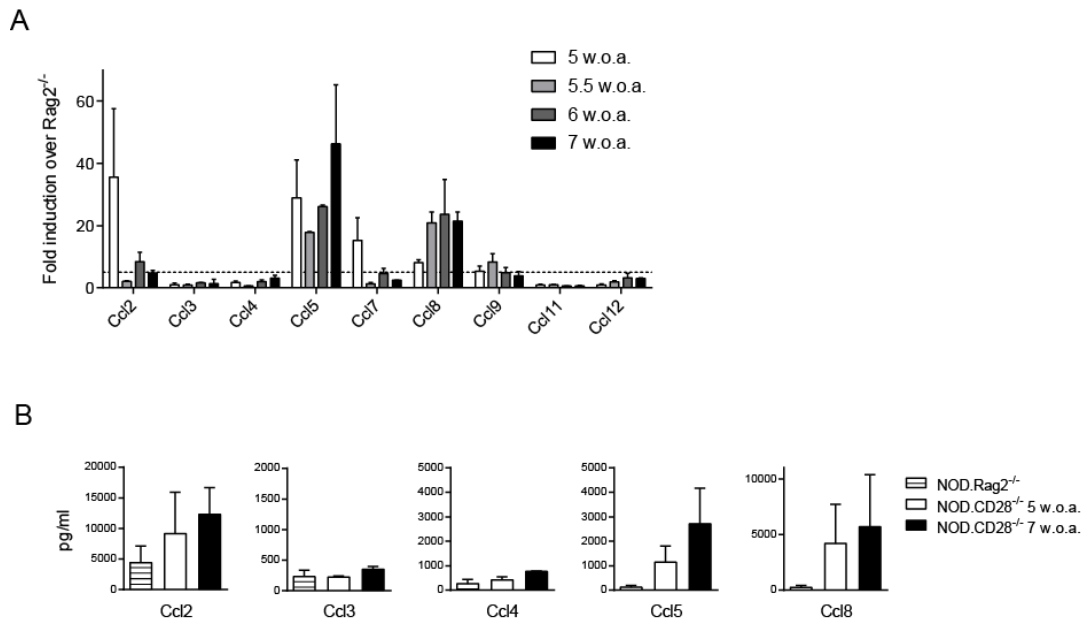
Figure 2. CC-family chemokines are highly induced in inflamed islets.

(**A**) mRNA was isolated from pooled islets of NOD.Rag2$^{-/-}$ and of pre-diabetic

NOD.CD28$^{-/-}$ mice at various ages. Transcript levels of a panel of CC-family

chemokines were measured as part of a qRT-PCR array. Bar graph depicts the fold

induction of CC-family chemokines in NOD.CD28$^{-/-}$ islets as compared to NOD.Rag2$^{-/-}$

islets. Only those chemokines that were expressed at detectable levels in NOD.CD28$^{-/-}$

islets (Ct < 30) are shown. Dashed line represents a 5-fold increase. Bars depict mean

fold-change + SEM from 2 independent experiments with 4-5 mice pooled per group in

each experiment. w.o.a., weeks of age. (**B**) Isolated islets from NOD.Rag2$^{-/-}$ and pre-

diabetic 5 and 7 week old NOD.CD28$^{-/-}$ mice were cultured overnight, homogenized, and

supernatants were analyzed for concentrations of monocyte-attracting chemokines. Bar

graphs depict mean + SEM from 2 independent experiments with 1-4 mice pooled per

group in each experiment.
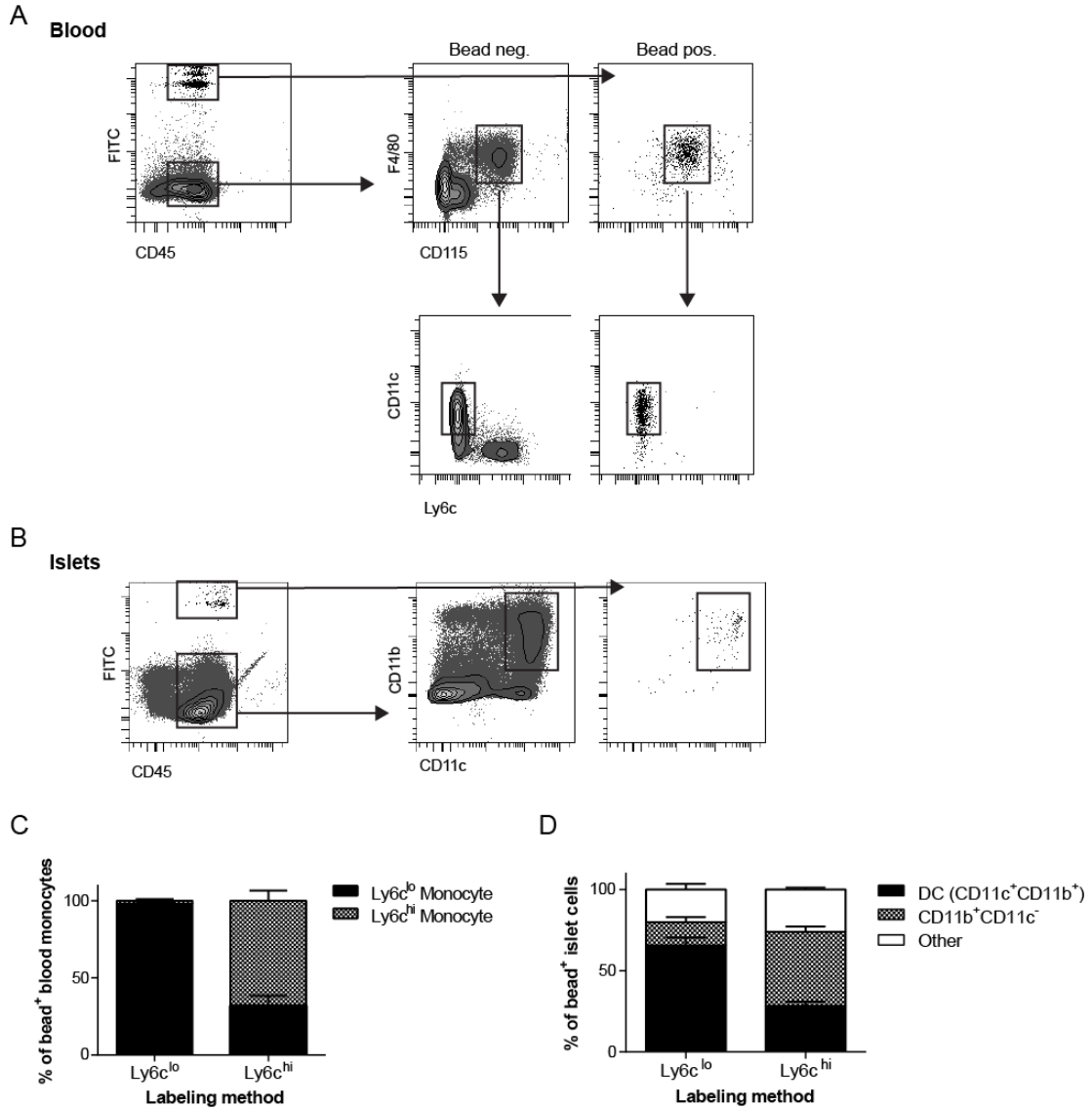
Figure 3. Islet DCs arise from Ly6c^{lo} blood monocytes.

(**A**) FITC-labeled latex beads were i.v. injected 3 d before analysis. Flow plots show that bead-labeled cells in the blood are primarily CD45$^+$F4/80$^+$CD115$^+$CD11c^{int}Ly6c^{lo} monocytes. (**B**) Bead-labeled cells in the corresponding islets are primarily CD45$^+$CD11c$^+$CD11b$^+$ DCs. Flow plots for A and B are from one representative mouse with greater than 10 mice examined. (**C**) Distribution of bead-labeled cells among blood monocytes at d5 post-bead injection using the Ly6c^{lo} labeling (bead injection alone) or

Ly6c labeling (pre-injection of clodronate liposomes 18h prior to bead injection) method.

(**D**) Distribution of bead-labeled cells in islets at d5 using the two different labeling methods in C. Data from C and D are from 7-8 mice per group from 2 independent experiments. Bars represent relative percentage of each population + SEM.
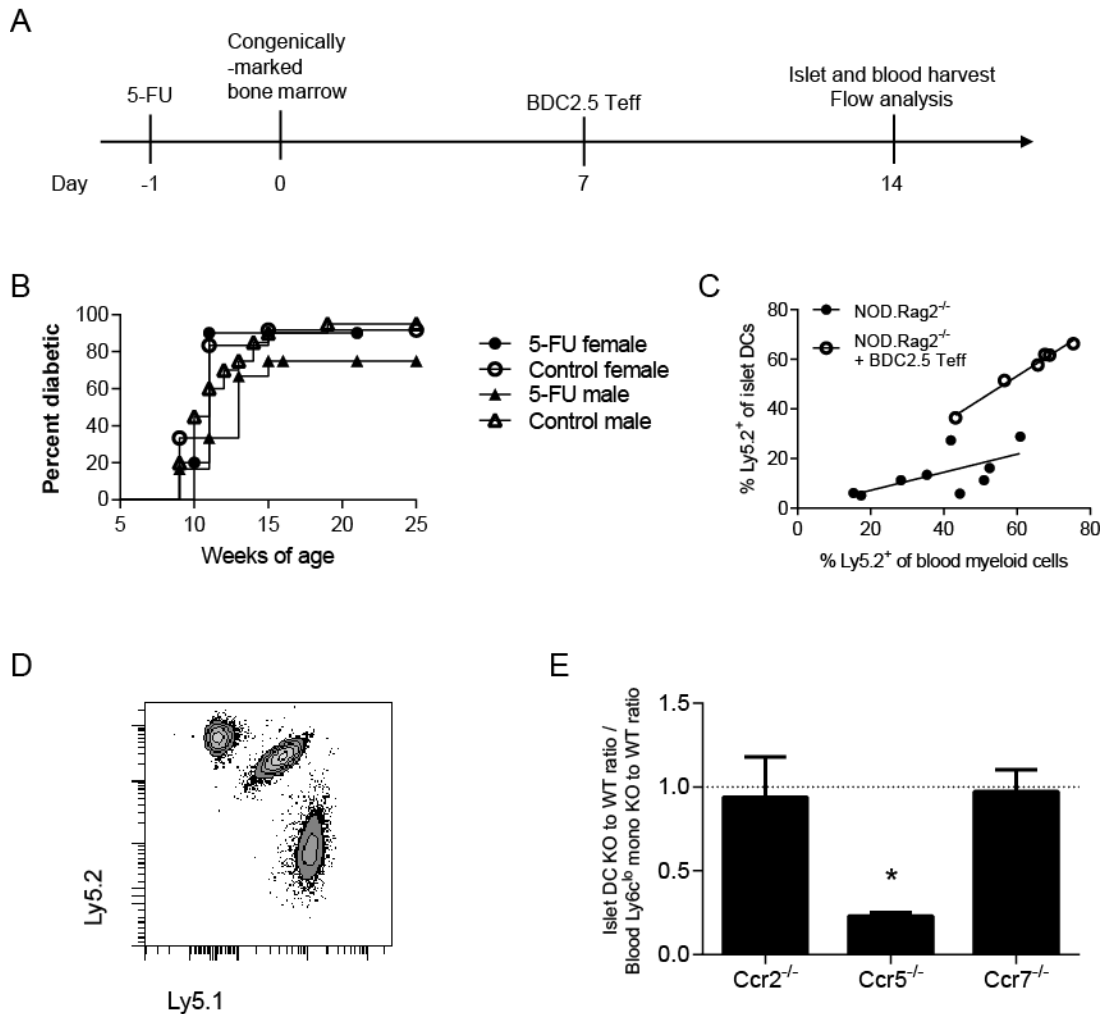
Figure 4. Islet DC recruitment is dependent on Ccr5.

(**A**) Schematic of the 5-FU protocol. NOD.Rag2$^{-/-}$ recipient mice are treated with 5-FU 1

d before receiving bone marrow cells from congenic Ly5.2 NOD.Rag2$^{-/-}$ donors. Some

mice received CD4$^+$CD25$^-$ BDC2.5 T cells on d 7 after bone marrow transplant to induce

islet inflammation. The percentage of Ly5.2$^+$ donor-derived monocytes in blood and

DCs in islets were determined by flow cytometry on d 14 after bone marrow transfer.

(**B**) 5-FU treatment at 5 to 6 weeks of age does not affect diabetes onset in NOD.CD28$^{-/-}$

mice. n=7-20 mice per group. (**C**) Scatter plot depicting the levels of peripheral versus

islet DC chimerism in NOD.Rag2$^{-/-}$.Ly5.1 mice treated as in (B) and receiving donor

bone marrow from NOD.Rag2$^{-/-}$.Ly5.2 mice. Each point represents one individual

mouse. Data is combined from 3 independent experiments. Difference in elevation

between groups, p<0.0001. (**D and E**) NOD.Rag2$^{-/-}$.Ly5.1/Ly5.2 mice were treated with

5-FU 1 d prior to receiving an equal mixture of bone marrow from wild-type B6.Ly5.1

and indicated chemokine receptor knockout B6.Ly5.2 mice. Mice received CD4$^+$CD25$^-$

BDC2.5 T cells on d 7 after bone marrow transplant to induce islet inflammation. (**D**)

Representative flow plot gated on DAPI$^-$Thy1.1$^-$CD4$^-$CD11c$^+$CD11b$^+$ islet DCs that are

made up of a mixture of endogenous- (Ly5.1$^+$Ly5.2$^+$), wild-type donor- (Ly5.1$^+$Ly5.2$^-$),

and chemokine receptor knockout donor- (Ly5.1$^-$Ly5.2$^+$) derived cells. (**E**) The

percentage of Ly5.1$^+$ wild-type donor-derived and Ly5.2$^+$ knockout donor-derived Ly6c^{lo}

monocytes in blood and of DCs in islets was determined by flow cytometry on d 14 after

bone marrow transfer.   The ratio of knockout to wild-type donor islet DCs was

determined and divided by the ratio of knockout to wild-type donor blood Ly6c^{lo}

monocytes. No difference in chimerism between blood and islets would be a value of 1.

Bar graphs represent mean + SEM of 2-4 mice per group from 2 independent

experiments. *, P < 0.05 for a one sample t test of value difference from 1.
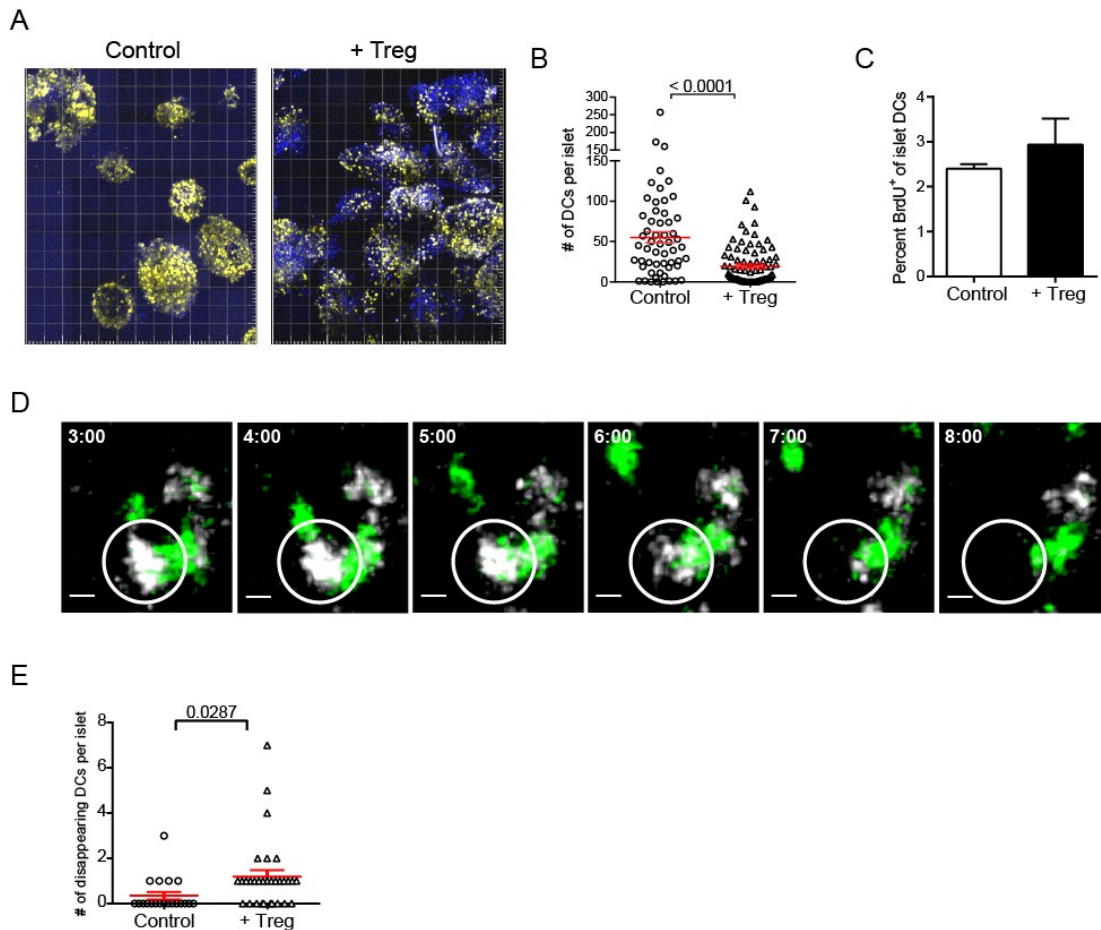
Figure 5. BDC2.5 Tregs reduce endogenous islet DC numbers.

(**A and B**) NOD.CD28$^{-/-}$.CD11c-YFP mice were treated with BDC2.5 Tregs at 5 weeks

of age. Two weeks later, isolated islets from treated mice and untreated age-matched

littermates were imaged by two-photon microscopy. (**A**) Maximal projection images

depicting compiled fields of view containing multiple islets isolated from control (left)

and BDC2.5 Treg-treated (right) mice. Nuclei labeled were labeled with Hoechst (blue)

and CD11c-YFP$^+$ DCs are displayed in yellow. (**B**) Quantification of the number of DCs

per islet. Each point represents one islet from a total of 4 mice per group imaged over 2

independent experiments. P value determined by Student's t test. (**C**) Proliferation of

islet DCs was measured by BrdU incorporation following a 4 h BrdU pulse two weeks

after BDC2.5 Treg treatment. Islet DCs were gated as $CD45^+CD11c^+B220^-$. Bar graph depicts mean + SEM of 3 mice per group from one experiment. (**D**) Maximal projection timelapse images taken at 1 min intervals depicting the disappearance of a YFP^+ DC (white, circled) following contact with BDC2.5 Tregs (green). Scale bar represents 5 um. (**E**) Quantification of the number of disappearing DCs observed during each 20-30 min imaging period. Each dot represents 1 islet from 3-4 mice imaged per group. Bars represent mean + SEM. P value determined by Student's t test.
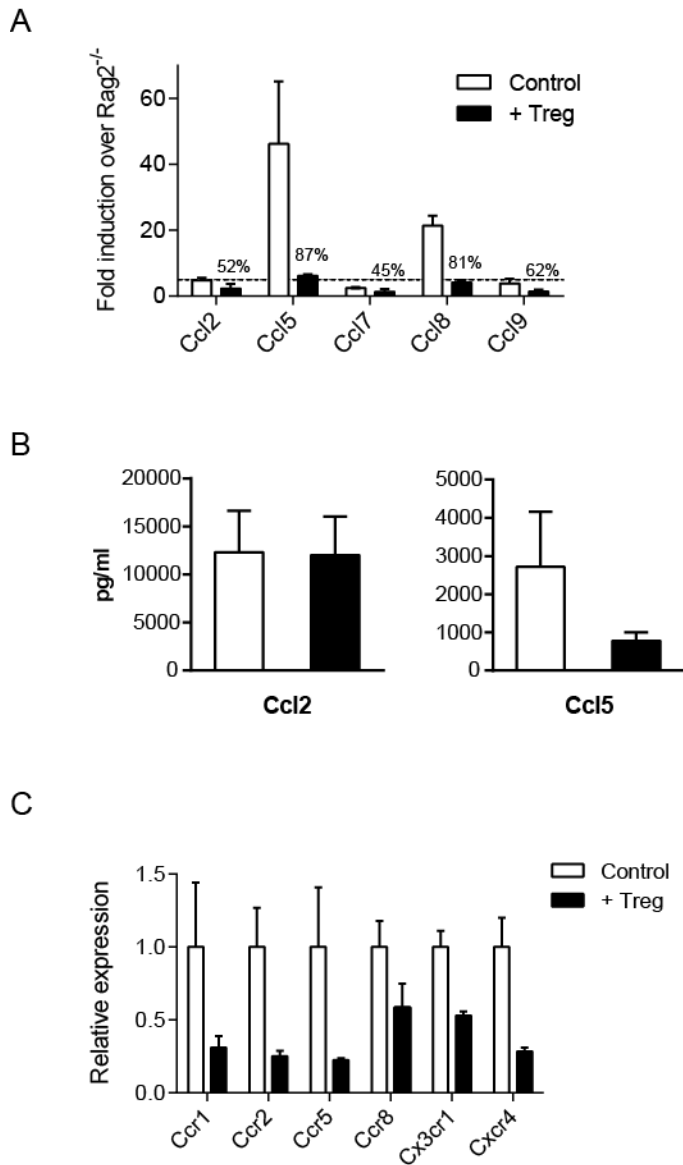
Figure 6. Downregulation of DC-attracting chemokines following BDC2.5 Treg treatment.

(**A**) mRNA was isolated from pooled islets isolated from female NOD.CD28$^{-/-}$ mice that had been either treated or not with BDC2.5 Tregs 2 weeks earlier and analyzed by qPCR array. Bar graph depicts expression relative to non-inflamed NOD.Rag2-/- control islets for CC-family chemokines that were shown to be upregulated in inflamed islets in Figure 1B.   Bars depict mean fold-change + SEM from 2 independent experiments. Dashed line

represents a 5-fold change. (**B**) Isolated islets from mice Treg-treated as above were cultured overnight and homogenized, and supernatants were analyzed for chemokine proteins. Graphs are mean + SEM of 2 independent experiments for Ccl2 and Ccl5, one experiment for Ccl8, samples run in duplicate. (**C**) Chemokine receptors expressed by monocytes were downregulated in Treg-treated mice. Transcript levels were measured as part of the qPCR array described in (A). Data represents mean fold-change + SEM from 2 independent experiments. Dashed line represents a 5-fold change.
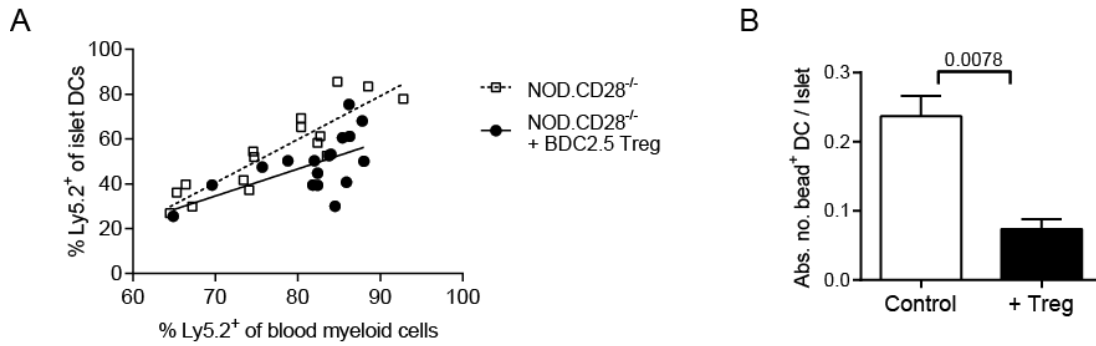
Figure 7. BDC2.5 Tregs reduce DC recruitment to islets.

(**A**) NOD.CD28$^{-/-}$ mice were treated with 5-FU as in Fig. 2, 1 d before receiving a bone

marrow transfer from NOD.Rag2$^{-/-}$.Ly5.2 donors with or without 2 x 10^6 BDC2.5 Tregs.

Analysis was performed at day 14 after transfer. Data is combined from 4 independent

experiments. Difference in elevation between groups, p=0.0009. (**B**) NOD.CD28$^{-/-}$ mice

that were either treated or not with BDC2.5 Tregs 2 weeks earlier were i.v. injected with

FITC-labeled latex beads. 3 d later, the number of bead$^+$ DCs per islet was enumerated

by flow. Data is from 1 of 2 representative experiments, with 3 mice per group in each

experiment. P value was determined by Student's t test.

CHAPTER IV. CONCLUSIONS AND FUTURE DIRECTIONS

Summary

This work has highlighted the many levels at which Tregs function in the tissue during an ongoing autoimmune response to exert their suppressive effects. We have seen that Tregs halt disease progression through their effects on multiple immune cell types. Immediately upon their arrival in the tissue, Tregs actively engage with resident DCs, as observed by two-photon microscopy. $CD8^+$ T cell recruitment to the islets is quickly reduced, leading to a rapid and specific decrease of these cells in the tissue. Tregs also rapidly suppress the effector function of those T cells that remain in the islets, both $CD4^+$ and $CD8^+$. This suppression occurs at the post-transcriptional level, as IFNγ protein but not message levels are reduced by Tregs. In $CD8^+$ T cells, this suppression correlates with a decrease in mTOR signaling that is required for their sustained production of IFNγ protein. These early alterations in the islet inflammatory milieu are followed by the establishment of a maintenance status in the tissue, where a reduced but persistent immune infiltrate is prevented from causing further beta cell destruction. This maintenance phase is characterized by decreased expression of inflammatory chemokines in the islets at the transcriptional level and a corresponding decrease in the recruitment of $Ly6c^{lo}$ monocytes, the precursors of islet DCs, into the tissue. This results in an eventual reduction in numbers of these disease-propagating DCs.

87

Treg suppression of effector CD8^{+} T cells: A metabolic mechanism?

In investigating the mechanisms of how Tregs suppress islet CD8^{+} T cells, we have discovered an inhibition of mTOR signaling in CD8^{+} T cells following Treg treatment. This finding hints at the possibility that Tregs may suppress effector T cells at a metabolic level as a means of exerting their suppressive functions, but fully demonstrating this was beyond the scope of this work. Going forward, additional evidence must be gathered to validate the conclusion that Tregs suppress effector T cell metabolic function, both at additional levels of the cell signaling pathway, and in settings other than Treg treatment of NOD.CD28^{-/-} mice. The literature provides some suggestions of where to look in the metabolic pathways of CD8^{+} T cells. The Pearce group has recently demonstrated that effector T cell cytokine production, but not proliferation, is dependent on aerobic glycolysis. When aerobic glycolysis was blocked in activated T cells, their production of IFNγ was inhibited at the translational level (Chang et al., 2013). This state of arrest is very similar to that observed in our model of Treg suppression *in vivo*, suggesting that perhaps Tregs are disrupting the glycolytic pathway of effector T cells. Of note, the Pearce study focused only on CD4^{+} T cells, so whether CD8^{+} T cells exhibit the same dependency on aerobic glycolysis for effector function remains to be determined. A relevant study on the metabolism of CD8^{+} T cells recently published by the Cantrell group shows that mTOR signaling is critical to maintain glycolysis in CD8^{+} T cells (Finlay et al., 2012). This control over glycolysis was mediated by mTOR regulation of expression of the transcription factor complex HIF1. As mTOR signaling was suppressed in CD8^{+} T cells in our model, this again

suggests that Tregs may suppress aerobic glycolysis in effector T cells. The work of Finlay et al. directs us to look at islet CD8^{+} T cell expression of HIF1 following Treg suppression, as well as expression of key glycolytic enzymes and glucose transporters that were demonstrated to be transcriptionally regulated by HIF1, including: glucose transporter 1 (Glut 1), hexokinase 2, phosphofructokinase 1, pyruvate kinases, and lactate dehydrogenase. An observed decrease in these molecules in islet T cells following Treg treatment at either the transcriptional or post-transcriptional level would strengthen the evidence that Tregs suppress by disrupting the glycolytic pathway in effector T cells.

Another remaining question is the upstream events that would lead to this alteration in T cell metabolism. mTOR has been shown to be activated by PI3K − AKT signaling. CD28 costimulation is a strong activator of PI3K signaling (Garcon et al., 2008; Sanchez-Lockhart et al., 2004). This could be cause for concern, as our observations that Tregs suppress mTOR in CD8^{+} T cells have been made in NOD.CD28^{-/-} mice whose T cells lack CD28 costimulation. This lack of CD28 costimulation could render mTOR suppression in these cells more achievable than would otherwise be the case in wild-type cells. However, Finlay et al. showed that PI3K- and Akt-independent pathways mediated the mTOR-HIF1 activation that was required for CD8^{+} T cell glycolysis, suggesting that the lack of CD28 costimulation in our model system might not be a major factor in our observations. Nonetheless, it will be important to test whether the same Treg suppression of effector T cell mTOR activation is observed in other experimental models. One such model is the NOD.Foxp3-DTR mouse. Preliminary experiments have shown that Treg depletion by diphtheria toxin administration in these

mice leads to a selective increase in islet CD8$^+$ T cells. Future experiments will examine

whether this is accompanied by a concomitant increase in mTOR signaling in these cells.

Also of value to pursuing this question will be the development of an *in vitro*

system to show that this method of Treg suppression can be recapitulated in general co-

culture settings. An *in vitro* model will also aid in dissecting this suppression at a more

mechanistic level by making cell numbers less limiting than they are in the tissue and by

making the cells easier to directly manipulate. Current efforts in the lab are going into

developing this system. Tregs are added in culture to pre-activated splenocytes to mimic

the ongoing inflammation at the time of Treg treatment of our *in vivo* disease model.

Initial experiments have shown that Tregs are capable of suppressing IFNγ production in

the *in vitro* co-culture system without impeding T cell proliferation, mimicking our *in*

vivo observations. Further experiments will test the metabolic properties of these

suppressed T cells using an extracellular flux analyzer.

This *in vitro* culture system will also aid in answering the question of whether our

observed Treg suppression of CD8$^+$ effector T cells is direct or indirect. This has been a

frequent question over the course of this work, as Tregs are commonly considered as

suppressors of CD4$^+$ helper T cells first and foremost. Indeed, Tregs suppress IFNγ

production similarly in both CD4$^+$ and CD8$^+$ T cells in the islets. A possible example of

indirect suppression of CD8$^+$ T cells would be if Tregs directly suppress CD4$^+$ T cells,

which in turn produce less IL-2 that is critical to the CD8$^+$ T cells. However, work in our

in vitro islet culture system did not robustly demonstrate a dependency on IL-2 or other

common gamma chain cytokines to maintain islet T cell IFNγ production. This suggests

that suppression of CD4$^+$ T cell help might not be the primary means of shutting down

CD8$^+$ effector function. If this is the case, Treg suppression of CD8$^+$ T cells might be more direct. While initial studies in our *in vitro* culture system are using whole splenocytes as responder cells, further work will investigate the ability of Tregs to suppress activated CD8$^+$ T cells in isolation. Previous work in this area has shown that Tregs suppress CD8$^+$ T cells directly in an *in vitro* co-culture in a manner that is independent of APCs or CD4$^+$ T cells and that is not reversed by the addition of IL-2 (Piccirillo and Shevach, 2001). In these studies, Tregs suppressed both T cell proliferation and IFNγ production; however, CD8$^+$ T cells were activated at the same time as Tregs were added to the culture. Our studies will address whether and how Tregs suppress effector CD8$^+$ T cells when the CD8$^+$ T cells are pre-activated prior to the addition of Tregs.

Targeting DCs in T1D

Our finding that Tregs target tissue DCs in autoimmune diabetes further implicates these cells as important contributors to disease pathogenesis. This raises the question of whether therapies that target these cells should be considered for the treatment or prevention of T1D. Having determined that DCs in inflamed islets of NOD mice arise from a Ly6c^{lo} monocyte precursor, it would be of use to determine if DCs in the islets of T1D patients are derived from the human equivalent. The human equivalents of mouse Ly6c^{hi} and Ly6c^{lo} monocytes are CD14^{++}CD16$^-$ and CD14$^+$CD16$^+$, respectively, with the CD14^{++}CD16$^-$ subset comprising ~90% of the total blood

monocyte population (Shi and Pamer, 2011). While the relative frequency of CD14^{+} monocytes in the peripheral blood does not differ between sero-negative and sero-positive first-degree relatives of T1D patients, possible differences specifically in the smaller CD16^{+} monocyte population in at-risk or recent onset T1D patients have not been investigated (Alkanani et al., 2012). Elevated frequencies of CD16^{+} monocytes have been detected in patients with rheumatoid arthritis (Kawanaka et al., 2002). A similar increase in T1D patients might suggest that these cells are systemically mobilized for recruitment to the tissue and differentiation into DCs, which might recommend them for targeting in the periphery before their arrival in the tissue.

In our studies, the impact of Treg treatment on DCs was restricted to DCs located in the inflamed tissue, with negligible impact on DCs in the draining lymph nodes. This suggests that tissue DCs are especially important to target in order to control disease progression. In other studies however, when depletion of DCs in NOD mice has resulted in disease protective effects, such depletion has been systemic (Nikolic et al., 2005; Saxena et al., 2007). A highly valuable tool in further dissecting the contribution of islet DCs to disease pathogenesis would be the ability to specifically target tissue DCs without affecting those in the draining LN.

At the current time, our two-photon imaging studies have focused on DC-T cell interactions in isolated islets. While these studies are very helpful in revealing cell-cell interactions within the tissue, they do not allow for visualization of cell entry from the periphery. Collaborative efforts between our lab and the Friedman and Krummel labs have led to the development of a method for intravital imaging of the islets *in situ* in the pancreas of a living mouse. The Friedman group has further developed this approach to

image T cell entry into and dynamics within inflamed islets, but this approach could also be applied to imaging the recruitment of islet DCs. A useful tool in such studies would be the Cx3cr1-GFP transgenic mouse. GFP is expressed in monocytes, NK cell and some T cells in these mice. As Ly6c^{lo} but not Ly6c^{hi} monocytes preferentially express Cx3cr1, the Ly6c^{lo} subset is especially bright for GFP in these mice (Auffray et al., 2007). Also, islet DCs under steady-state conditions are GFP^{+} in these mice, lending further evidence that monocytes are the islet DC precursors in steady-state conditions (Zhang et al., 2009). Intravital pancreas imaging using these mice under steady-state and inflammatory conditions would allow a unique means of visualizing the recruitment of these cells into the islets.

In our model, recruitment of DCs to the islets is partially dependent on Ccr5, with inflamed islets expressing high levels of the Ccr5 ligand Ccl5. The cellular source of this Ccl5 within inflamed islets and the identity of the cells that downregulate Ccl5 following Treg treatment remains to be determined, but previous reports have found Ccl5 to be expressed by beta cells (Carvalho-Pinto et al., 2004). As the continued presence of islet DCs appears to be important in propagating islet inflammation, targeting Ccr5 to block the entry of these cells into the tissue might be a means of inhibiting disease progression. At the same time, one should bear in mind that the change in islet chemokine expression and corresponding reduction in DC recruitment was not immediate. Thus, while targeting this recruitment may aid in maintaining immune quiescence in conjunction with other therapies, it may not be sufficient to prevent or reverse disease on its own.

<u>Outlook</u>

      As Tregs begin to enter the clinic for their first trials as therapeutic treatments for autoimmune patients and transplant recipients, much remains to be understood about their biology. The work presented in this dissertation has contributed to our understanding of Treg function by examining the effects of therapeutic Tregs on multiple immune cell types in a setting of chronic autoimmunity. Our studies have highlighted the importance of Treg function within the target tissue, serving as another reminder of the limitations of the conclusions to be drawn from studies of peripheral blood in human patients. Although difficult to track in human patients, this ability of Tregs to home to the site of inflammation and exert localized suppression will be a great advantage of this and other potential cellular therapies over systemically administered small molecule and biologic drugs. The extent to which this localization ability is dependent on the antigen specificity of the Tregs should be taken into consideration, and may push for the use of antigen specific Tregs in patients, despite the difficulties of such an approach over using polyclonal Tregs. The multiple cellular targets and the multiple levels at which these cells are targeted by Tregs as seen in this work suggest that many of the various mechanisms that have been ascribed to Treg function likely operate in concert to suppress the progression of a complex autoimmune disease. The ability of Tregs to work in this multi-faceted manner is yet another reason these cells hold strong therapeutic potential. How well the reality of Tregs in the clinic will fulfill their pre-clinical promise remains to be seen; but this path is surely one to be followed with cautious optimism, as many new insights into immune regulation will be discovered along the way.

REFERENCES

Akbar, A.N., N.J. Borthwick, R.G. Wickremasinghe, P. Panayoitidis, D. Pilling, M. Bofill, S. Krajewski, J.C. Reed, and M. Salmon. 1996. Interleukin-2 receptor common gamma-chain signaling cytokines regulate activated T cell apoptosis in response to growth factor withdrawal: selective induction of anti-apoptotic (bcl-2, bcl-xL) but not pro-apoptotic (bax, bcl-xS) gene expression. *Eur J Immunol* 26:294-299.

Alkanani, A.K., M. Rewers, F. Dong, K. Waugh, P.A. Gottlieb, and D. Zipris. 2012. Dysregulated Toll-like receptor-induced interleukin-1beta and interleukin-6 responses in subjects at risk for the development of type 1 diabetes. *Diabetes* 61:2525-2533.

Anderson, M.S., and J.A. Bluestone. 2005a. The NOD mouse: a model of immune dysregulation. *Annu Rev Immunol* 23:447-485.

Anderson, M.S., and J.A. Bluestone. 2005b. The NOD mouse: a model of immune dysregulation. *Annu Rev Immunol* 23:447-485.

Araki, K., A.P. Turner, V.O. Shaffer, S. Gangappa, S.A. Keller, M.F. Bachmann, C.P. Larsen, and R. Ahmed. 2009. mTOR regulates memory CD8 T-cell differentiation. *Nature* 460:108-112.

Auffray, C., D. Fogg, M. Garfa, G. Elain, O. Join-Lambert, S. Kayal, S. Sarnacki, A. Cumano, G. Lauvau, and F. Geissmann. 2007. Monitoring of blood vessels and tissues by a population of monocytes with patrolling behavior. *Science* 317:666-670.

Birnberg, T., L. Bar-On, A. Sapoznikov, M.L. Caton, L. Cervantes-Barragan, D. Makia, R. Krauthgamer, O. Brenner, B. Ludewig, D. Brockschnieder, D. Riethmacher, B. Reizis, and S. Jung. 2008. Lack of conventional dendritic cells is compatible with normal development and T cell homeostasis, but causes myeloid proliferative syndrome. *Immunity* 29:986-997.

Bresson, D., L. Togher, E. Rodrigo, Y. Chen, J.A. Bluestone, K.C. Herold, and M. von Herrath. 2006. Anti-CD3 and nasal proinsulin combination therapy enhances remission from recent-onset autoimmune diabetes by inducing Tregs. *The Journal of clinical investigation* 116:1371-1381.

Bromley, S.K., S.Y. Thomas, and A.D. Luster. 2005. Chemokine receptor CCR7 guides T cell exit from peripheral tissues and entry into afferent lymphatics. *Nature immunology* 6:895-901.

Brunkow, M.E., E.W. Jeffery, K.A. Hjerrild, B. Paeper, L.B. Clark, S.A. Yasayko, J.E. Wilkinson, D. Galas, S.F. Ziegler, and F. Ramsdell. 2001. Disruption of a new forkhead/winged-helix protein, scurfin, results in the fatal lymphoproliferative disorder of the scurfy mouse. *Nature genetics* 27:68-73.

Brunstein, C.G., J.S. Miller, Q. Cao, D.H. McKenna, K.L. Hippen, J. Curtsinger, T. Defor, B.L. Levine, C.H. June, P. Rubinstein, P.B. McGlave, B.R. Blazar, and J.E. Wagner. 2011. Infusion of ex vivo expanded T regulatory cells in adults transplanted with umbilical cord blood: safety profile and detection kinetics. *Blood* 117:1061-1070.

Brusko, T., C. Wasserfall, K. McGrail, R. Schatz, H.L. Viener, D. Schatz, M. Haller, J. Rockell, P. Gottlieb, M. Clare-Salzler, and M. Atkinson. 2007. No alterations in the frequency of FOXP3+ regulatory T-cells in type 1 diabetes. *Diabetes* 56:604-612.

Brusko, T.M., C.H. Wasserfall, M.J. Clare-Salzler, D.A. Schatz, and M.A. Atkinson. 2005. Functional defects and the influence of age on the frequency of CD4+ CD25+ T-cells in type 1 diabetes. *Diabetes* 54:1407-1414.

Calderon, B., A. Suri, M.J. Miller, and E.R. Unanue. 2008. Dendritic cells in islets of Langerhans constitutively present beta cell-derived peptides bound to their class II MHC molecules. *Proc Natl Acad Sci U S A* 105:6121-6126.

Cao, X., S.F. Cai, T.A. Fehniger, J. Song, L.I. Collins, D.R. Piwnica-Worms, and T.J. Ley. 2007. Granzyme B and perforin are important for regulatory T cell-mediated suppression of tumor clearance. *Immunity* 27:635-646.

Carvalho-Pinto, C., M.I. Garcia, L. Gomez, A. Ballesteros, A. Zaballos, J.M. Flores, M. Mellado, J.M. Rodriguez-Frade, D. Balomenos, and A.C. Martinez. 2004. Leukocyte attraction through the CCR5 receptor controls progress from insulitis to diabetes in non-obese diabetic mice. *Eur J Immunol* 34:548-557.

CDC. 2011. National diabetes fact sheet: national estimates and general information on diabetes and prediabetes in the United States, 2011. In D.o.H.a.H. Services, editor Centers for Disease Control and Prevention, Atlanta, GA: U.S.

Chang, C.H., J.D. Curtis, L.B. Maggi, Jr., B. Faubert, A.V. Villarino, D. O'Sullivan, S.C. Huang, G.J. van der Windt, J. Blagih, J. Qiu, J.D. Weber, E.J. Pearce, R.G. Jones, and E.L. Pearce. 2013. Posttranscriptional control of T cell effector function by aerobic glycolysis. *Cell* 153:1239-1251.

Chen, Z., A.E. Herman, M. Matos, D. Mathis, and C. Benoist. 2005. Where CD4+CD25+ T reg cells impinge on autoimmune diabetes. *The Journal of experimental medicine* 202:1387-1397.

Collison, L.W., C.J. Workman, T.T. Kuo, K. Boyd, Y. Wang, K.M. Vignali, R. Cross, D. Sehy, R.S. Blumberg, and D.A. Vignali. 2007. The inhibitory cytokine IL-35 contributes to regulatory T-cell function. *Nature* 450:566-569.

Coppieters, K.T., F. Dotta, N. Amirian, P.D. Campbell, T.W. Kay, M.A. Atkinson, B.O. Roep, and M.G. von Herrath. 2012. Demonstration of islet-autoreactive CD8 T cells in insulitic lesions from recent onset and long-term type 1 diabetes patients. *The Journal of experimental medicine* 209:51-60.

Darrasse-Jeze, G., S. Deroubaix, H. Mouquet, G.D. Victora, T. Eisenreich, K.H. Yao, R.F. Masilamani, M.L. Dustin, A. Rudensky, K. Liu, and M.C. Nussenzweig. 2009. Feedback control of regulatory T cell homeostasis by dendritic cells in vivo. *The Journal of experimental medicine* 206:1853-1862.

Debes, G.F., C.N. Arnold, A.J. Young, S. Krautwald, M. Lipp, J.B. Hay, and E.C. Butcher. 2005. Chemokine receptor CCR7 required for T lymphocyte exit from peripheral tissues. *Nature immunology* 6:889-894.

Delgoffe, G.M., T.P. Kole, Y. Zheng, P.E. Zarek, K.L. Matthews, B. Xiao, P.F. Worley, S.C. Kozma, and J.D. Powell. 2009. The mTOR kinase differentially regulates effector and regulatory T cell lineage commitment. *Immunity* 30:832-844.

Delgoffe, G.M., K.N. Pollizzi, A.T. Waickman, E. Heikamp, D.J. Meyers, M.R. Horton, B. Xiao, P.F. Worley, and J.D. Powell. 2011. The kinase mTOR regulates the

differentiation of helper T cells through the selective activation of signaling by mTORC1 and mTORC2. *Nature immunology* 12:295-303.

Di Ianni, M., F. Falzetti, A. Carotti, A. Terenzi, F. Castellino, E. Bonifacio, B. Del Papa, T. Zei, R.I. Ostini, D. Cecchini, T. Aloisi, K. Perruccio, L. Ruggeri, C. Balucani, A. Pierini, P. Sportoletti, C. Aristei, B. Falini, Y. Reisner, A. Velardi, F. Aversa, and M.F. Martelli. 2011. Tregs prevent GVHD and promote immune reconstitution in HLA-haploidentical transplantation. *Blood* 117:3921-3928.

Edelson, B.T., W. Kc, R. Juang, M. Kohyama, L.A. Benoit, P.A. Klekotka, C. Moon, J.C. Albring, W. Ise, D.G. Michael, D. Bhattacharya, T.S. Stappenbeck, M.J. Holtzman, S.S. Sung, T.L. Murphy, K. Hildner, and K.M. Murphy. 2010. Peripheral CD103+ dendritic cells form a unified subset developmentally related to CD8alpha+ conventional dendritic cells. *The Journal of experimental medicine* 207:823-836.

Feuerer, M., Y. Shen, D.R. Littman, C. Benoist, and D. Mathis. 2009. How punctual ablation of regulatory T cells unleashes an autoimmune lesion within the pancreatic islets. *Immunity* 31:654-664.

Finlay, D.K., E. Rosenzweig, L.V. Sinclair, C. Feijoo-Carnero, J.L. Hukelmann, J. Rolf, A.A. Panteleyev, K. Okkenhaug, and D.A. Cantrell. 2012. PDK1 regulation of mTOR and hypoxia-inducible factor 1 integrate metabolism and migration of CD8+ T cells. *The Journal of experimental medicine* 209:2441-2453.

Fontenot, J.D., M.A. Gavin, and A.Y. Rudensky. 2003. Foxp3 programs the development and function of CD4+CD25+ regulatory T cells. *Nature immunology* 4:330-336.

Ganguly, D., S. Haak, V. Sisirak, and B. Reizis. 2013. The role of dendritic cells in autoimmunity. *Nature reviews. Immunology* 13:566-577.

Garcon, F., D.T. Patton, J.L. Emery, E. Hirsch, R. Rottapel, T. Sasaki, and K. Okkenhaug. 2008. CD28 provides T-cell costimulation and enhances PI3K activity at the immune synapse independently of its capacity to interact with the p85/p110 heterodimer. *Blood* 111:1464-1471.

Gasteiger, G., S. Hemmers, P.D. Bos, J.C. Sun, and A.Y. Rudensky. 2013a. IL-2-dependent adaptive control of NK cell homeostasis. *The Journal of experimental medicine*

Gasteiger, G., S. Hemmers, M.A. Firth, A. Le Floc'h, M. Huse, J.C. Sun, and A.Y. Rudensky. 2013b. IL-2-dependent tuning of NK cell sensitivity for target cells is controlled by regulatory T cells. *The Journal of experimental medicine*

Geissmann, F., S. Jung, and D.R. Littman. 2003. Blood monocytes consist of two principal subsets with distinct migratory properties. *Immunity* 19:71-82.

Geissmann, F., M.G. Manz, S. Jung, M.H. Sieweke, M. Merad, and K. Ley. 2010. Development of monocytes, macrophages, and dendritic cells. *Science* 327:656-661.

Ginhoux, F., K. Liu, J. Helft, M. Bogunovic, M. Greter, D. Hashimoto, J. Price, N. Yin, J. Bromberg, S.A. Lira, E.R. Stanley, M. Nussenzweig, and M. Merad. 2009. The origin and development of nonlymphoid tissue CD103+ DCs. *The Journal of experimental medicine* 206:3115-3130.

Grossman, W.J., J.W. Verbsky, W. Barchet, M. Colonna, J.P. Atkinson, and T.J. Ley. 2004. Human T regulatory cells can use the perforin pathway to cause autologous target cell death. *Immunity* 21:589-601.

Hori, S., T. Nomura, and S. Sakaguchi. 2003. Control of regulatory T cell development by the transcription factor Foxp3. *Science* 299:1057-1061.

Hu, C.Y., D. Rodriguez-Pinto, W. Du, A. Ahuja, O. Henegariu, F.S. Wong, M.J. Shlomchik, and L. Wen. 2007. Treatment with CD20-specific antibody prevents and reverses autoimmune diabetes in mice. *The Journal of clinical investigation* 117:3857-3867.

Hu, J.K., T. Kagari, J.M. Clingan, and M. Matloubian. 2011. Expression of chemokine receptor CXCR3 on T cells affects the balance between effector and memory CD8 T-cell generation. *Proc Natl Acad Sci U S A* 108:E118-127.

Jakubzick, C., M. Bogunovic, A.J. Bonito, E.L. Kuan, M. Merad, and G.J. Randolph. 2008a. Lymph-migrating, tissue-derived dendritic cells are minor constituents within steady-state lymph nodes. *The Journal of experimental medicine* 205:2839-2850.

Jakubzick, C., F. Tacke, F. Ginhoux, A.J. Wagers, N. van Rooijen, M. Mack, M. Merad, and G.J. Randolph. 2008b. Blood monocyte subsets differentially give rise to CD103+ and CD103- pulmonary dendritic cell populations. *J Immunol* 180:3019-3027.

Jansen, A., F. Homo-Delarche, H. Hooijkaas, P.J. Leenen, M. Dardenne, and H.A. Drexhage. 1994. Immunohistochemical characterization of monocytes-macrophages and dendritic cells involved in the initiation of the insulitis and beta-cell destruction in NOD mice. *Diabetes* 43:667-675.

Kawanaka, N., M. Yamamura, T. Aita, Y. Morita, A. Okamoto, M. Kawashima, M. Iwahashi, A. Ueno, Y. Ohmoto, and H. Makino. 2002. CD14+,CD16+ blood monocytes and joint inflammation in rheumatoid arthritis. *Arthritis and rheumatism* 46:2578-2586.

Khattri, R., T. Cox, S.A. Yasayko, and F. Ramsdell. 2003. An essential role for Scurfin in CD4+CD25+ T regulatory cells. *Nature immunology* 4:337-342.

Kim, J.M., J.P. Rasmussen, and A.Y. Rudensky. 2007. Regulatory T cells prevent catastrophic autoimmunity throughout the lifespan of mice. *Nature immunology* 8:191-197.

Lawson, J.M., J. Tremble, C. Dayan, H. Beyan, R.D. Leslie, M. Peakman, and T.I. Tree. 2008. Increased resistance to CD4+CD25hi regulatory T cell-mediated suppression in patients with type 1 diabetes. *Clinical and experimental immunology* 154:353-359.

Lee, L.F., K. Logronio, G.H. Tu, W. Zhai, I. Ni, L. Mei, J. Dilley, J. Yu, A. Rajpal, C. Brown, C. Appah, S.M. Chin, B. Han, T. Affolter, and J.C. Lin. 2012. Anti-IL-7 receptor-alpha reverses established type 1 diabetes in nonobese diabetic mice by modulating effector T-cell function. *Proc Natl Acad Sci U S A* 109:12674-12679.

Lenschow, D.J., Y. Zeng, K.S. Hathcock, L.A. Zuckerman, G. Freeman, J.R. Thistlethwaite, G.S. Gray, R.J. Hodes, and J.A. Bluestone. 1995. Inhibition of transplant rejection following treatment with anti-B7-2 and anti-B7-1 antibodies. *Transplantation* 60:1171-1178.

Lindley, S., C.M. Dayan, A. Bishop, B.O. Roep, M. Peakman, and T.I. Tree. 2005. Defective suppressor function in CD4(+)CD25(+) T-cells from patients with type 1 diabetes. *Diabetes* 54:92-99.

Liu, F., and J.L. Whitton. 2005. Cutting edge: re-evaluating the in vivo cytokine responses of CD8+ T cells during primary and secondary viral infections. *J Immunol* 174:5936-5940.

Liu, K., G.D. Victora, T.A. Schwickert, P. Guermonprez, M.M. Meredith, K. Yao, F.F. Chu, G.J. Randolph, A.Y. Rudensky, and M. Nussenzweig. 2009. In vivo analysis of dendritic cell development and homeostasis. *Science* 324:392-397.

Long, S.A., K. Cerosaletti, P.L. Bollyky, M. Tatum, H. Shilling, S. Zhang, Z.Y. Zhang, C. Pihoker, S. Sanda, C. Greenbaum, and J.H. Buckner. 2010. Defects in IL-2R signaling contribute to diminished maintenance of FOXP3 expression in CD4(+)CD25(+) regulatory T-cells of type 1 diabetic subjects. *Diabetes* 59:407-415.

Long, S.A., M. Rieck, S. Sanda, J.B. Bollyky, P.L. Samuels, R. Goland, A. Ahmann, A. Rabinovitch, S. Aggarwal, D. Phippard, L.A. Turka, M.R. Ehlers, P.J. Bianchine, K.D. Boyle, S.A. Adah, J.A. Bluestone, J.H. Buckner, and C.J. Greenbaum. 2012. Rapamycin/IL-2 combination therapy in patients with type 1 diabetes augments Tregs yet transiently impairs beta-cell function. *Diabetes* 61:2340-2348.

Ma, D.Y., and E.A. Clark. 2009. The role of CD40 and CD154/CD40L in dendritic cells. *Seminars in immunology* 21:265-272.

Marek-Trzonkowska, N., M. Mysliwiec, A. Dobyszuk, M. Grabowska, I. Techmanska, J. Juscinska, M.A. Wujtewicz, P. Witkowski, W. Mlynarski, A. Balcerska, J. Mysliwska, and P. Trzonkowski. 2012. Administration of CD4+CD25highCD127- regulatory T cells preserves beta-cell function in type 1 diabetes in children. *Diabetes care* 35:1817-1820.

McGonagle, D., and M.F. McDermott. 2006. A proposed classification of the immunological diseases. *PLoS medicine* 3:e297.

McNally, A., G.R. Hill, T. Sparwasser, R. Thomas, and R.J. Steptoe. 2011. CD4+CD25+ regulatory T cells control CD8+ T-cell effector differentiation by modulating IL-2 homeostasis. *Proc Natl Acad Sci U S A* 108:7529-7534.

Medina, M.A., J. Couturier, M.L. Feske, A.E. Mahne, M. Turner, X. Yu, C.A. Kozinetz, A.F. Orozco, A.T. Hutchison, T.C. Savidge, J.R. Rodgers, and D.E. Lewis. 2012. Granzyme B- and Fas ligand-mediated cytotoxic function induced by mitogenic CD28 stimulation of human memory CD4+ T cells. *Journal of leukocyte biology* 91:759-771.

Melli, K., R.S. Friedman, A.E. Martin, E.B. Finger, G. Miao, G.L. Szot, M.F. Krummel, and Q. Tang. 2009. Amplification of autoimmune response through induction of dendritic cell maturation in inflamed tissues. *J Immunol* 182:2590-2600.

Mempel, T.R., M.J. Pittet, K. Khazaie, W. Weninger, R. Weissleder, H. von Boehmer, and U.H. von Andrian. 2006. Regulatory T cells reversibly suppress cytotoxic T cell function independent of effector differentiation. *Immunity* 25:129-141.

Miller, J.C., B.D. Brown, T. Shay, E.L. Gautier, V. Jojic, A. Cohain, G. Pandey, M. Leboeuf, K.G. Elpek, J. Helft, D. Hashimoto, A. Chow, J. Price, M. Greter, M. Bogunovic, A. Bellemare-Pelletier, P.S. Frenette, G.J. Randolph, S.J. Turley, and M. Merad. 2012. Deciphering the transcriptional network of the dendritic cell lineage. *Nature immunology* 13:888-899.

Nguyen, V.T., and E.N. Benveniste. 2000. Involvement of STAT-1 and ets family members in interferon-gamma induction of CD40 transcription in microglia/macrophages. *The Journal of biological chemistry* 275:23674-23684.

Nikolic, T., S.B. Geutskens, N. van Rooijen, H.A. Drexhage, and P.J. Leenen. 2005. Dendritic cells and macrophages are essential for the retention of lymphocytes in (peri)-insulitis of the nonobese diabetic mouse: a phagocyte depletion study. *Lab Invest* 85:487-501.

Onishi, Y., Z. Fehervari, T. Yamaguchi, and S. Sakaguchi. 2008. Foxp3+ natural regulatory T cells preferentially form aggregates on dendritic cells in vitro and actively inhibit their maturation. *Proc Natl Acad Sci U S A* 105:10113-10118.

Pandiyan, P., L. Zheng, S. Ishihara, J. Reed, and M.J. Lenardo. 2007. CD4(+)CD25(+)Foxp3(+) regulatory T cells induce cytokine deprivation-mediated apoptosis of effector CD4(+) T cells. *Nat Immunol* 8:1353-1362.

Pearce, E.L., M.C. Walsh, P.J. Cejas, G.M. Harms, H. Shen, L.S. Wang, R.G. Jones, and Y. Choi. 2009. Enhancing CD8 T-cell memory by modulating fatty acid metabolism. *Nature* 460:103-107.

Penaranda, C., W. Kuswanto, J. Hofmann, R. Kenefeck, P. Narendran, L.S. Walker, J.A. Bluestone, A.K. Abbas, and H. Dooms. 2012. IL-7 receptor blockade reverses autoimmune diabetes by promoting inhibition of effector/memory T cells. *Proc Natl Acad Sci U S A* 109:12668-12673.

Pescovitz, M.D., C.J. Greenbaum, H. Krause-Steinrauf, D.J. Becker, S.E. Gitelman, R. Goland, P.A. Gottlieb, J.B. Marks, P.F. McGee, A.M. Moran, P. Raskin, H. Rodriguez, D.A. Schatz, D. Wherrett, D.M. Wilson, J.M. Lachin, and J.S. Skyler. 2009. Rituximab, B-lymphocyte depletion, and preservation of beta-cell function. *The New England journal of medicine* 361:2143-2152.

Piccirillo, C.A., and E.M. Shevach. 2001. Cutting edge: control of CD8+ T cell activation by CD4+CD25+ immunoregulatory cells. *J Immunol* 167:1137-1140.

Powell, J.D., K.N. Pollizzi, E.B. Heikamp, and M.R. Horton. 2012. Regulation of immune responses by mTOR. *Annu Rev Immunol* 30:39-68.

Putnam, A.L., T.M. Brusko, M.R. Lee, W. Liu, G.L. Szot, T. Ghosh, M.A. Atkinson, and J.A. Bluestone. 2009. Expansion of human regulatory T-cells from patients with type 1 diabetes. *Diabetes* 58:652-662.

Putnam, A.L., F. Vendrame, F. Dotta, and P.A. Gottlieb. 2005. CD4+CD25high regulatory T cells in human autoimmune diabetes. *Journal of autoimmunity* 24:55-62.

Qureshi, O.S., Y. Zheng, K. Nakamura, K. Attridge, C. Manzotti, E.M. Schmidt, J. Baker, L.E. Jeffery, S. Kaur, Z. Briggs, T.Z. Hou, C.E. Futter, G. Anderson, L.S. Walker, and D.M. Sansom. 2011. Trans-endocytosis of CD80 and CD86: a molecular basis for the cell-extrinsic function of CTLA-4. *Science* 332:600-603.

Rao, R.R., Q. Li, K. Odunsi, and P.A. Shrikant. 2010. The mTOR kinase determines effector versus memory CD8+ T cell fate by regulating the expression of transcription factors T-bet and Eomesodermin. *Immunity* 32:67-78.

Rivollier, A., J. He, A. Kole, V. Valatas, and B.L. Kelsall. 2012. Inflammation switches the differentiation program of Ly6Chi monocytes from antiinflammatory macrophages to inflammatory dendritic cells in the colon. *The Journal of experimental medicine* 209:139-155.

Sakaguchi, S. 2004. Naturally arising CD4+ regulatory t cells for immunologic self-tolerance and negative control of immune responses. *Annu Rev Immunol* 22:531-562.

Sakaguchi, S., N. Sakaguchi, M. Asano, M. Itoh, and M. Toda. 1995. Immunologic self-tolerance maintained by activated T cells expressing IL-2 receptor alpha-chains (CD25). Breakdown of a single mechanism of self-tolerance causes various autoimmune diseases. *J Immunol* 155:1151-1164.

Salomon, B., D.J. Lenschow, L. Rhee, N. Ashourian, B. Singh, A. Sharpe, and J.A. Bluestone. 2000. B7/CD28 costimulation is essential for the homeostasis of the CD4+CD25+ immunoregulatory T cells that control autoimmune diabetes. *Immunity* 12:431-440.

Sanchez-Lockhart, M., E. Marin, B. Graf, R. Abe, Y. Harada, C.E. Sedwick, and J. Miller. 2004. Cutting edge: CD28-mediated transcriptional and posttranscriptional regulation of IL-2 expression are controlled through different signaling pathways. *J Immunol* 173:7120-7124.

Santamaria, P. 2003. Kinetic evolution of a diabetogenic CD8+ T cell response. *Annals of the New York Academy of Sciences* 1005:88-97.

Satpathy, A.T., X. Wu, J.C. Albring, and K.M. Murphy. 2012. Re(de)fining the dendritic cell lineage. *Nature immunology* 13:1145-1154.

Saxena, V., J.K. Ondr, A.F. Magnusen, D.H. Munn, and J.D. Katz. 2007. The countervailing actions of myeloid and plasmacytoid dendritic cells control autoimmune diabetes in the nonobese diabetic mouse. *J Immunol* 179:5041-5053.

Schlecht, G., J. Mouries, M. Poitrasson-Riviere, C. Leclerc, and G. Dadaglio. 2006. Purification of splenic dendritic cells induces maturation and capacity to stimulate Th1 response in vivo. *International immunology* 18:445-452.

Schneider, A., M. Rieck, S. Sanda, C. Pihoker, C. Greenbaum, and J.H. Buckner. 2008. The effector T cells of diabetic subjects are resistant to regulation via CD4+ FOXP3+ regulatory T cells. *J Immunol* 181:7350-7355.

Serreze, D.V., H.D. Chapman, D.S. Varnum, M.S. Hanson, P.C. Reifsnyder, S.D. Richard, S.A. Fleming, E.H. Leiter, and L.D. Shultz. 1996. B lymphocytes are essential for the initiation of T cell-mediated autoimmune diabetes: analysis of a new "speed congenic" stock of NOD.Ig mu null mice. *The Journal of experimental medicine* 184:2049-2053.

Serreze, D.V., S.A. Fleming, H.D. Chapman, S.D. Richard, E.H. Leiter, and R.M. Tisch. 1998. B lymphocytes are critical antigen-presenting cells for the initiation of T cell-mediated autoimmune diabetes in nonobese diabetic mice. *J Immunol* 161:3912-3918.

Shi, C., and E.G. Pamer. 2011. Monocyte recruitment during infection and inflammation. *Nature reviews. Immunology* 11:762-774.

Shinomiya, M., S. Nadano, H. Shinomiya, and M. Onji. 2000. In situ characterization of dendritic cells occurring in the islets of nonobese diabetic mice during the development of insulitis. *Pancreas* 20:290-296.

Sitrin, J., A. Ring, K.C. Garcia, C. Benoist, and D. Mathis. 2013. Regulatory T cells control NK cells in an insulitic lesion by depriving them of IL-2. *The Journal of experimental medicine*

Solomon, M., B. Balasa, and N. Sarvetnick. 2010. CCR2 and CCR5 chemokine receptors differentially influence the development of autoimmune diabetes in the NOD mouse. *Autoimmunity* 43:156-163.

Tacke, F., D. Alvarez, T.J. Kaplan, C. Jakubzick, R. Spanbroek, J. Llodra, A. Garin, J. Liu, M. Mack, N. van Rooijen, S.A. Lira, A.J. Habenicht, and G.J. Randolph. 2007. Monocyte subsets differentially employ CCR2, CCR5, and CX3CR1 to accumulate within atherosclerotic plaques. *The Journal of clinical investigation* 117:185-194.

Tacke, F., F. Ginhoux, C. Jakubzick, N. van Rooijen, M. Merad, and G.J. Randolph. 2006. Immature monocytes acquire antigens from other cells in the bone marrow and present them to T cells after maturing in the periphery. *The Journal of experimental medicine* 203:583-597.

Tang, Q., J.Y. Adams, C. Penaranda, K. Melli, E. Piaggio, E. Sgouroudis, C.A. Piccirillo, B.L. Salomon, and J.A. Bluestone. 2008. Central role of defective interleukin-2 production in the triggering of islet autoimmune destruction. *Immunity* 28:687-697.

Tang, Q., J.Y. Adams, A.J. Tooley, M. Bi, B.T. Fife, P. Serra, P. Santamaria, R.M. Locksley, M.F. Krummel, and J.A. Bluestone. 2006. Visualizing regulatory T cell control of autoimmune responses in nonobese diabetic mice. *Nature immunology* 7:83-92.

Tang, Q., and J.A. Bluestone. 2006. Regulatory T-cell physiology and application to treat autoimmunity. *Immunological reviews* 212:217-237.

Tang, Q., and J.A. Bluestone. 2008. The Foxp3+ regulatory T cell: a jack of all trades, master of regulation. *Nature immunology* 9:239-244.

Tang, Q., K.J. Henriksen, M. Bi, E.B. Finger, G. Szot, J. Ye, E.L. Masteller, H. McDevitt, M. Bonyhadi, and J.A. Bluestone. 2004. In vitro-expanded antigen-specific regulatory T cells suppress autoimmune diabetes. *The Journal of experimental medicine* 199:1455-1465.

Tarbell, K.V., L. Petit, X. Zuo, P. Toy, X. Luo, A. Mqadmi, H. Yang, M. Suthanthiran, S. Mojsov, and R.M. Steinman. 2007. Dendritic cell-expanded, islet-specific CD4+ CD25+ CD62L+ regulatory T cells restore normoglycemia in diabetic NOD mice. *The Journal of experimental medicine* 204:191-201.

Tarbell, K.V., S. Yamazaki, K. Olson, P. Toy, and R.M. Steinman. 2004a. CD25+ CD4+ T cells, expanded with dendritic cells presenting a single autoantigenic peptide, suppress autoimmune diabetes. *J Exp Med* 199:1467-1477.

Tarbell, K.V., S. Yamazaki, K. Olson, P. Toy, and R.M. Steinman. 2004b. CD25+ CD4+ T cells, expanded with dendritic cells presenting a single autoantigenic peptide, suppress autoimmune diabetes. *The Journal of experimental medicine* 199:1467-1477.

Trzonkowski, P., M. Bieniaszewska, J. Juscinska, A. Dobyszuk, A. Krzystyniak, N. Marek, J. Mysliwska, and A. Hellmann. 2009. First-in-man clinical results of the treatment of patients with graft versus host disease with human ex vivo expanded CD4+CD25+CD127- T regulatory cells. *Clin Immunol* 133:22-26.

Tsou, C.L., W. Peters, Y. Si, S. Slaymaker, A.M. Aslanian, S.P. Weisberg, M. Mack, and I.F. Charo. 2007. Critical roles for CCR2 and MCP-3 in monocyte mobilization
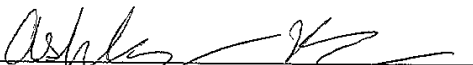
from bone marrow and recruitment to inflammatory sites. *The Journal of clinical investigation* 117:902-909.

Turley, S., L. Poirot, M. Hattori, C. Benoist, and D. Mathis. 2003. Physiological beta cell death triggers priming of self-reactive T cells by dendritic cells in a type-1 diabetes model. *The Journal of experimental medicine* 198:1527-1537.

van der Vliet, H.J., and E.E. Nieuwenhuis. 2007. IPEX as a result of mutations in FOXP3. *Clinical & developmental immunology* 2007:89017.

Varol, C., A. Vallon-Eberhard, E. Elinav, T. Aychek, Y. Shapira, H. Luche, H.J. Fehling, W.D. Hardt, G. Shakhar, and S. Jung. 2009. Intestinal lamina propria dendritic cell subsets have different origin and functions. *Immunity* 31:502-512.

Verdaguer, J., D. Schmidt, A. Amrani, B. Anderson, N. Averill, and P. Santamaria. 1997. Spontaneous autoimmune diabetes in monoclonal T cell nonobese diabetic mice. *The Journal of experimental medicine* 186:1663-1676.

Vignali, D.A., L.W. Collison, and C.J. Workman. 2008. How regulatory T cells work. *Nature reviews. Immunology* 8:523-532.

Villarino, A.V., S.D. Katzman, E. Gallo, O. Miller, S. Jiang, M.T. McManus, and A.K. Abbas. 2011. Posttranscriptional silencing of effector cytokine mRNA underlies the anergic phenotype of self-reactive T cells. *Immunity* 34:50-60.

Wang, B.G., A; Benoist, C; Mathis, D. 1996. CD8 role in T1D inititation. *Eur J Immunol*

Wen, X., T. Kudo, L. Payne, X. Wang, L. Rodgers, and Y. Suzuki. 2010. Predominant interferon-gamma-mediated expression of CXCL9, CXCL10, and CCL5 proteins in the brain during chronic infection with Toxoplasma gondii in BALB/c mice resistant to development of toxoplasmic encephalitis. *Journal of interferon & cytokine research : the official journal of the International Society for Interferon and Cytokine Research* 30:653-660.

Willcox, A., S.J. Richardson, A.J. Bone, A.K. Foulis, and N.G. Morgan. 2009. Analysis of islet inflammation in human type 1 diabetes. *Clinical and experimental immunology* 155:173-181.

Wing, K., Y. Onishi, P. Prieto-Martin, T. Yamaguchi, M. Miyara, Z. Fehervari, T. Nomura, and S. Sakaguchi. 2008. CTLA-4 control over Foxp3+ regulatory T cell function. *Science* 322:271-275.

Yamaguchi, T., J.B. Wing, and S. Sakaguchi. 2011. Two modes of immune suppression by Foxp3(+) regulatory T cells under inflammatory or non-inflammatory conditions. *Seminars in immunology* 23:424-430.

Yin, N., J. Xu, F. Ginhoux, G.J. Randolph, M. Merad, Y. Ding, and J.S. Bromberg. 2012. Functional specialization of islet dendritic cell subsets. *J Immunol* 188:4921-4930.

Zhang, N., B. Schroppel, G. Lal, C. Jakubzick, X. Mao, D. Chen, N. Yin, R. Jessberger, J.C. Ochando, Y. Ding, and J.S. Bromberg. 2009. Regulatory T cells sequentially migrate from inflamed tissues to draining lymph nodes to suppress the alloimmune response. *Immunity* 30:458-469.

Zhao, D.M., A.M. Thornton, R.J. DiPaolo, and E.M. Shevach. 2006. Activated CD4+CD25+ T cells selectively kill B lymphocytes. *Blood* 107:3925-3932.

Publishing Agreement

It is the policy of the University to encourage the distribution of all theses, dissertations, and manuscripts. Copies of all UCSF theses, dissertations, and manuscripts will be routed to the library via the Graduate Division. The library will make all theses, dissertations, and manuscripts accessible to the public and will preserve these to the best of their abilities, in perpetuity.

Please sign the following statement:

I hereby grant permission to the Graduate Division of the University of California, San Francisco to release copies of my thesis, dissertation, or manuscript to the Campus Library to provide access and preservation, in whole or in part, in perpetuity.

_____   _____
Author Signature   Date   8/29/13

104